

Copyright Warning & Restrictions

The copyright law of the United States (Title 17, United States Code) governs the making of photocopies or other reproductions of copyrighted material.

Under certain conditions specified in the law, libraries and archives are authorized to furnish a photocopy or other reproduction. One of these specified conditions is that the photocopy or reproduction is not to be “used for any purpose other than private study, scholarship, or research.” If a user makes a request for, or later uses, a photocopy or reproduction for purposes in excess of “fair use” that user may be liable for copyright infringement,

This institution reserves the right to refuse to accept a copying order if, in its judgment, fulfillment of the order would involve violation of copyright law.

Please Note: The author retains the copyright while the New Jersey Institute of Technology reserves the right to distribute this thesis or dissertation

Printing note: If you do not wish to print this page, then select “Pages from: first page # to: last page #” on the print dialog screen

The Van Houten library has removed some of the personal information and all signatures from the approval page and biographical sketches of theses and dissertations in order to protect the identity of NJIT graduates and faculty.

ABSTRACT

OPTICAL PROPERTIES OF POLYMERS AND THEIR APPLICATIONS

by

Samiha Hossain

The last decade has witnessed explosive growth in the world of photoactive polymers for a variety of applications in several sectors of the global economy. The need for efficient, reliable, and low-cost data acquisition, storage, processing, transmission, and display technologies has made it necessary for research aimed at addressing these needs. Recent accomplishments in this materials area represent exciting opportunities for major innovations in various fields. However, further work needs to be done to transfer the technology from fundamental R&D to manufacturing. The goal of this study is to provide a better understanding of the optical properties of polymers and identify the candidates that are ideal for a variety of applications.

The fundamental optical properties and characteristics of several commonly used polymers are presented in this study. Mathematical simulations of signal propagation through a polymer core waveguide are examined to determine the materials that are most suitable for long range communications. Other applications such as electronic devices, temperature and pressure sensors, protective coatings and energetic materials are briefly considered. Self-healing and self-repair in polymers are examined.

OPTICAL PROPERTIES OF POLYMERS AND THEIR APPLICATIONS

by

Samiha Hossain

A Thesis

Submitted to the Faculty of

New Jersey Institute of Technology

in Partial Fulfillment of the Requirements for the Degree of

Master of Science in Materials Science and Engineering

Interdisciplinary Program in Materials Science and Engineering

August 2019

Blank Page

APPROVAL PAGE

OPTICAL PROPERTIES OF POLYMERS AND THEIR APPLICATIONS

Samiha Hossain

Dr. Nuggehalli M. Ravindra, Thesis Advisor
Professor of Physics, NJIT

Date

Dr. Michael Jaffe, Committee Member
Research Professor of Biomedical Engineering, NJIT

Date

Dr. Sagnik Basuray, Committee Member
Assistant Professor, Chemical & Materials Engineering, NJIT

Date

BIOGRAPHICAL SKETCH

Author: Samiha Hossain
Degree: Master of Science
Date: August 2019

Undergraduate and Graduate Education:

- Master of Science in Materials Science and Engineering, New Jersey Institute of Technology, Newark, NJ, 2019
- Master of Science in Biomedical Engineering, New Jersey Institute of Technology, Newark, NJ, 2015
- Bachelor of Science in Biomedical Engineering, Rutgers University, School of Engineering, New Brunswick, NJ 2012

Major: Materials Science and Engineering

Publications and Presentations:

Samiha Hossain and N. M. Ravindra, "Self-Healing in Materials: An Overview," Proceedings of the 2019 TMS Annual Meeting & Exhibition, San Antonio, TX, pp. 1643-1661, March 2019

ACKNOWLEDGMENT

I would firstly like to thank my thesis advisor Dr. N. M. Ravindra for his continuous, energetic guidance, helpful constructive criticism and kind advice that directed me while I completed my thesis.

I would also like to thank Dr. Michael Jaffe and Dr. Sagnik Basuray for agreeing to be on my committee.

Lastly, I would like to express my sincerest gratitude to my peers, Jonathan Martinez, Airefetalo Sadoh and Anushua Arif for their contribution to the project. The countless hours they put in and their illuminating views on issues related to the project were invaluable for its completion.

TABLE OF CONTENTS

Chapter	Page
1 INTRODUCTION TO POLYMERS.....	1
1.1 Classification of Polymers.....	1
1.2 Physical Properties of Polymers.....	5
1.3 Mechanical Properties of Polymers.....	6
2 OPTICAL PROPERTIES: FUNDAMENTALS.....	8
2.1 Dielectric Constant.....	8
2.2 Refractive Index.....	9
2.3 Dispersion and Absorption.....	10
2.4 Relation to Dielectric Constant.....	11
2.5 Reflection.....	12
2.6 Absorption.....	13
2.7 Transmission.....	14
2.8 Emissivity.....	14
2.9 Kramers-Kronig Relations and the Cauchy Method.....	15
3 OPTICAL AND ELECTRICAL PROPERTIES OF POLYMERS.....	17
3.1 Behavior in a Steady (d.c.) Electric Field.....	17
3.2 Optical Properties.....	19
3.3 Color and Infrared Absorption.....	20
3.4 Refraction.....	21

TABLE OF CONTENTS
(Continued)

Chapter	Page
3.6 Transparency.....	22
4 FUNDAMENTALS OF DOPING OF POLYMERS.....	25
4.1 The Concept of Doping.....	25
4.2 Examples of the Effect of Doping on Optical Properties of Polymers...	26
4.3 Influence of Impurities on Optical Properties of Polymers.....	30
5 WAVEGUIDE FUNDAMENTALS.....	31
5.1 Optical Propagation.....	32
5.2 Boundary Conditions: Reflection and Transmission.....	37
6 SIMULATIONS.....	38
6.1 Description.....	38
7 RESULTS AND DISCUSSION.....	41
7.1 Poly(9,9-dioctylfluorene-alt-benzothiadiazole) (F8BT).....	41
7.2 Poly(methyl methacrylate) (PMMA).....	46
7.3 Poly(vinyl alcohol) (PVA).....	51
7.4 Polyaniline (PANI).....	55
8 APPLICATIONS AND FUTURE WORK.....	58
8.1 Sensors.....	58
8.2 Organic Photovoltaic (OPV) Solar Cells.....	64
8.3 Coatings.....	68
8.4 Energetic Materials.....	72

TABLE OF CONTENTS
(Continued)

Chapter		Page
8.5	Future Work.....	73
9	REFERENCES.....	75

LIST OF TABLES

Table		Page
1.1	U.S. Production of Major Plastics and Synthetic Fibers in 2012	2
1.2	Chemical Structure of Repeating Units of Commonly Used Polymers	4
7.1	F8BT Max and Min Values of its Transmission Spectra	44
7.2	PMMA Waveguide Max and Min Values of its Transmission Spectra	49
7.3	PVA Waveguide Max and Min Values of its Transmission Spectra ...	52
8.1	Examples of Different Types of Polymeric Gas Sensors	61
8.2	Different Types of Polymeric Biosensors	63

LIST OF FIGURES

Figure		Page
1.1	Division of polymers based on thermal response	2
1.2	Synthesis of nylon-6,6 by condensation polymerization	4
3.1	a) Reflection and (b) scattering of light on transmission through a transparent medium, (c) Haze produced by wide-angle forward scattering of light, (d) Gloss: (from the top) specular reflection; perfect diffuse reflection; intermediate behavior. The polar envelope shows the angular distribution of reflected light intensity.....	24
4.1	(a) Normalized absorbance of PVC/NiO nanocomposites films and (b) Transmittance spectra of these nanocomposites	26
4.2	FTIR spectra of the pure and the VO ²⁺ (1, 2, 3, 4, and 5 mol%) doped PVP polymer electrolyte films	27
4.3	Absorption spectra of the pure and the VO ²⁺ (1, 2, 3, 4, and 5 mol%) doped PVP polymer electrolyte.....	27
4.4	The absorption spectra in the UV–VIS region for films of PVA/PPY and that doped with (0.2, 0.4, 0.6, 0.8 and 1.0 g of CoCl ₂ 6H ₂ O).....	28
4.5	The variation of transmittance for (PVP-KBr) composite vs wavelength.....	28
4.6	The variation of optical absorbance for (PVP-KBr) composite vs wavelength.....	29
4.7	The variation of optical absorption for PS-PMMA composite doped with NaF.....	29
5.1	Snell’s Law of Refraction	33
5.2	Total Internal Reflection	34
5.3	Slab Waveguide	35
5.4	Fiber Optic Propagation	36
7.1	Chemical Structure of F8BT	42

LIST OF FIGURES
(Continued)

Figure	Page
7.2 Transmittance spectra of CAISWG (green dash dot dot line), QISWG (blue short dash), ARWG (red solid line), SRWG (black dash line) and the used CA substrate (purple short dash dot) from study	42
7.3 Schematic of proposed system with F8BT as core and Cellulose Acetate as clad	43
7.4 Simulated transmittance spectra of Pure F8BT waveguide and Cellulose Acetate cladding	43
7.5 Simulated transmission spectra of F8BT waveguide system with a variety of materials as clad and core	45
7.6 Signal loss of NIST suggested wavelengths in IR-range in F8BT waveguide (core) with Cellulose Acetate clad vs length (distance travelled)	46
7.7 Chemical structure of PMMA	47
7.8 Schematic of proposed waveguide systems involving PMMA	47
7.9 Simulated transmission spectra of PMMA waveguide as cladding and Air and SiO ₂ as core	48
7.10 Signal loss of NIST suggested wavelengths in IR- range in waveguides with PMMA and SiO ₂ /Air systems vs length (distance travelled)	50
7.11 Chemical structure of PVA	51
7.12 Schematic of proposed waveguide systems involving PVA	51
7.13 Simulated transmission spectra of PVA waveguide as core and SiO ₂ as clad and Air as core and PVA as clad	52
7.14 Signal loss of NIST suggested wavelengths in IR- range in waveguides with PVA and SiO ₂ /Air systems vs length (distance travelled)	54
7.15 Molecular structure of the repeating unit for PANI-B	55

LIST OF FIGURES
(Continued)

Figure		Page
7.16	Schematic of of proposed waveguide systems involving PVA	56
7.17	Simulated transmission spectra of PANI waveguide as clad and SiO ₂ and Air as core	56
7.18	Signal loss of NIST suggested wavelengths in IR- range in waveguides with PVA and SiO ₂ /Air systems vs length (distance travelled)	57
8.1	Schematic color changes of an extended sample used to make stress sensors	62
8.2	Principles of operation of a biosensor	63
8.3	Schematic illustration of polymer solar cells can be manufactured by standard. printing processes	65
8.4	A comparison of the originally proposed bilayer cell, and the modern bulk heterojunction cell	66
8.5	An approximation of charge carrier transport in the full stack of a conventional OPV, using the organic molecule BCP as an ETL. The smooth movement of energy levels facilitating transport is known as a bandgap cascade	67
8.6	Laboratory OPV cells manufactured on glass	68
8.7	Lifetime extension of engineered materials by implementation of self-healing principle	71
8.8	Schematic of self-healing process. a) Self-healing coating containing microencapsulated catalyst (yellow) and phase-separated healing agent droplets (blue) in a matrix (light orange) on a metallic substrate (grey). b) Damage to the coating layer releases catalyst (green) and healing agent (blue). c) Mixing of healing agent and catalyst in the damaged region. d) Damage healed by cross-linked PDMS, protecting the substrate from the environment	72

CHAPTER 1

INTRODUCTION TO POLYMERS

The term polymer originates from the Greek word poly (meaning many) and mere (meaning parts). Basically, a polymer is a long chain molecule composed of repeating units of identical structure usually connected with covalent bonds. They can either be found naturally (e.g. proteins, cellulose, silk) or produced synthetically like in the case of nylon, polystyrene and polyethylene. Polymers are useful in different industries for various applications as they are cost-effective, easily accessible, largely nontoxic (mostly biodegradable) and malleable (Fried, 2014).

The birth of polymers and rise of polymer science in industry first began in the nineteenth century. Goodyear developed a vulcanization process which involved turning the natural rubber elastomer into tires. Next, the first manmade thermoplastic was developed in the 1860s. A century later, high performance polymer plastics were developed and were able to compete constructively with other more traditional materials in the automotive and aerospace industry. More recently, polymers with electrically conducting, photo conducting and liquid crystalline properties have been developed. As of today, polymeric materials have seeped into almost all aspects of our daily lives. Table 1.1 displays the amount of such polymers (plastics and synthetic fibers) produced in the United States in 2012.

1.1 Classification of Polymers

Polymers can be classified into different sub groups which include the following:

Thermal response, mechanism of polymerization, and polymer structure.

Table 1.1 U.S. Production of Major Plastics and Synthetic Fibers in 2012

PLASTICS	Thousands of Metric Tons	Annual Change (%) 2002-12
Polyethylene		
Low-density	3123	-1.5
Linear low-density	8098	1.7
High density	8046	1.1
Polypropylene	7405	-0.4
Polystyrene	2473	-2.0
PVC & copolymers	6944	0.0

All polymers can be classified into two major groups based on their thermal processing behavior. Polymers that can be melted and then processed into their desired form are referred to as thermoplastics. Recovered waste thermoplastics can be reused and repurposed using heat and pressure.

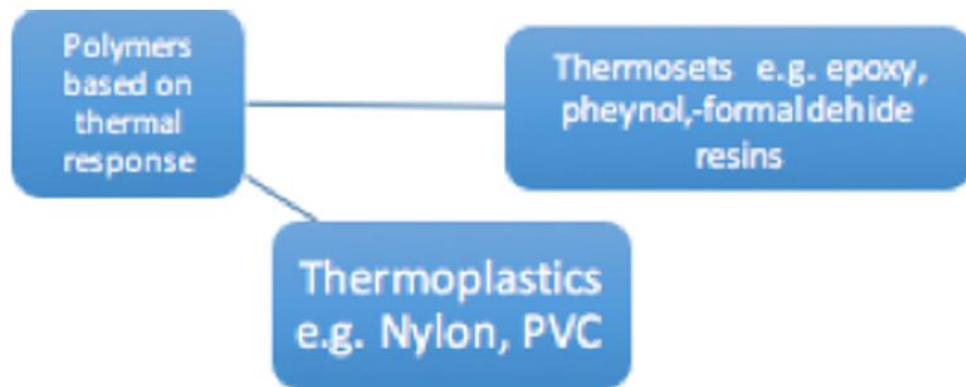


Figure 1.1 Classification of polymers based on thermal response.

Comparatively, thermosets are polymers whose individual chains are chemically linked by covalent bonds during chemical treatment or successive thermal treatments usually during fabrication. Once formed, these types of polymers are resistant to heat as well as mechanical deformation but cannot be thermally processed thereby making them excellent candidates for adhesives and coatings.

Wallace Carothers first classified polymers into either addition or condensation polymers depending on the mechanism of polymerization. Polystyrene, which is polymerized by a successive addition of styrene monomers, is an example of an addition polymer. Most important addition polymers are polymerized using olefins and vinyl-based monomers.

Other polymers belonging to the addition class are polymerized not by addition to an ethylene double bond but through a ring-opening polymerization of a sterically strained cyclic monomer. One such example is the ring-opening polymerization of trioxane to form polyoxymethylene (an engineering thermoplastic).

Table 1.2 lists the chemical structure of repeating units and the commonly used nomenclature of some of the most important addition-type polymers derived from substituted ethylene.

Condensation Polymers are obtained when two molecules randomly react. A molecule participating in a polycondensation reaction may be either a monomer, oligomer, or higher-molecular-weight intermediate with complementary functional end units, such as carboxylic acid or hydroxyl groups. Normally, condensation polymerizations occur by the release of a small molecule in the form of a gas, water, or salt. Any high-yield condensation reaction can be used to obtain a high-molecular-weight polymer. An example of a

condensation polymerization is the synthesis of nylon-6,6 by the polycondensation of adipic acid and hexamethylenediamine. This is illustrated in Figure 1.2.

Table 1.2 Chemical Structure of Repeating Units of Commonly Used Polymers

Polymer	R ₁	R ₂	R ₃	R ₄	Repeating Unit
Polyethylene	H	H	H	H	$\text{[-CH}_2\text{-CH}_2\text{-]}$
Polypropylene	H	H	H	CH ₃	$\text{[-CH}_2\text{-CH-]}$ CH ₃
Poly(vinyl chloride)	H	H	H	Cl	$\text{[-CH}_2\text{-CH-]}$ Cl

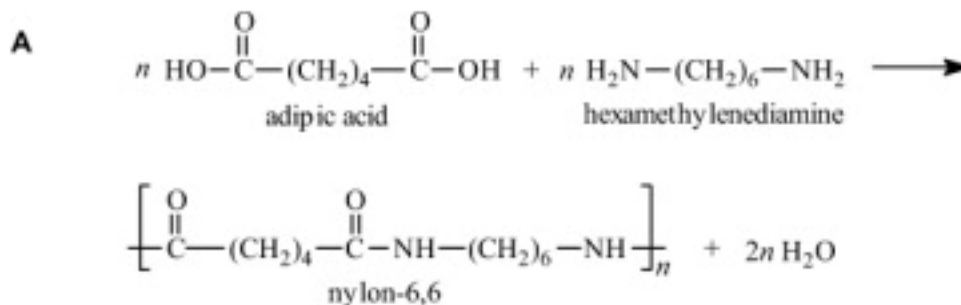


Figure 1.2 Synthesis of nylon-6,6 by condensation polymerization.

In addition to the mentioned classification based on processing and polymerization characteristics, polymers can also be grouped based on the chemical structure of their backbones. For example, polymers consisting all carbon atoms along their backbone are referred to as homochain polymers. Furthermore, they may be classified depending on whether there are single or double bonds along their backbone. Carbon-chain polymers

with only single bonds along the backbone are called *polyalkylenes* (or polyalkylidenes). Carbon-chain polymers with double bonds along the chain such as the diene elastomers—polyisoprene and polybutadiene—are called *polyalkenylenes*. Conversely, heterochain polymers contain more than one atom type in their backbone and are grouped according to the types of atoms and chemical groups (e.g., carbonyl, amide, or ester) located along the backbone (Fried, 2016).

1.2 Physical Properties of Polymers

The physical properties of polymers include molecular weight, melting point and glass transition temperature.

The molecular weight of a polymer molecule is the product of the degree of polymerization and the molecular weight of the repeating unit. The degree of polymerization in a polymer molecule is the number of repeating units in the polymer chain. Since the polymer molecules are not identical but usually a mixture of many species with dissimilar degrees of polymerization and consequently different molecular weights, most values of the molecular weight of a polymer is based on an average.

Polymers may be either amorphous or semi crystalline in nature. The amorphous region of a polymer is often witnessed at lower temperatures where the molecules of the polymer can vibrate slightly but do not move significantly. This state is often referred as the glassy state. In this state, the polymer is brittle, hard and rigid, similar to glass. However, when the polymer is heated, the polymer chains are able to wiggle around each other thereby becoming soft and flexible analogous to rubber. This state is called the rubbery state. The glass transition temperature (T_g) is the temperature at which the glassy

state makes the transition to the rubbery state. The glass transition temperature is the property of the amorphous region of the polymer, while the crystalline region is characterized by the melting point. Although, amorphous polymers do not have the melting point, all polymers have a glass transition temperature. Also, the melting point of a polymer is increased if double bonds, aromatic groups, bulky or large side groups are present in the polymer chain as a result of restriction in the flexibility of the chain. Conversely, the branching of chains causes the reduction in melting point because of defects that are produced by branching (Namazi, 2017).

1.3 Mechanical Properties of Polymers

Polymers are used in various aspects of our daily lives. As a result, it is necessary to be familiar with some of their mechanical properties before they are used in applications and products. Some basic questions need to be considered such as how much it can be stretched or bent, how hard or soft it is, how it behaves on the application of repeated load. These properties are considered below.

The strength of a material is determined by the stress required to cause a break. There are numerous types of strength, namely tensile (stretching of the polymer), compressional (compressing the polymer), flexural (bending of the polymer), torsional (twisting of the polymer), impact (hammering).

Strain is measured by the percentage change in the length of the material before fracture. It is also a measure of ductility.

Young's Modulus (Modulus of Elasticity or Tensile Modulus) is the ratio of stress to the strain in the linearly elastic region. Elastic modulus is a measure of the stiffness of the material. $E = \text{Tensile Stress}(\sigma) / \text{Tensile Strain}(\varepsilon)$.

The toughness of a material is typically determined using the area under the stress and strain curve. It typically measures the energy absorbed by the material before it breaks.

When considering viscoelasticity, there are two types of deformations: elastic and viscous. In elastic deformation, the strain is produced at the moment the constant load (or stress) is applied, and this strain is maintained until the stress is not released. Eliminating the stress allows the material to revert to its original dimensions completely. The deformation in this case is reversible. In the case of viscous deformation, the "damage" is irreversible as the material does not revert to its original dimensions. This kind of deformation is time dependent and the strain increases under constant load. Usually, polymers show a combined behavior of both elastic and plastic deformation which is dependent on the temperature and strain rate. At low temperature and high strain rate, elastic behavior is observed, and at high temperature but low strain rate, the viscous behavior is observed. A combination of viscous and elastic behavior is observed at intermediate temperature and strain rate values. This behavior is characterized as viscoelasticity, and the polymer which exhibits this behavior is referred to as viscoelastic (Balani et. al. 2015)

CHAPTER 2

OPTICAL PROPERTIES: FUNDAMENTALS

2.1 Dielectric Constant

A dielectric material can store electrical charge and thus can develop an electric field with minimum loss of energy. While polymers have traditionally been recognized as insulating materials and are used to insulate wires and electrical equipment, they also have dielectric properties. In practice, dielectric materials are composed of inorganic substances such as mica and silicon dioxide. However, polymers are quickly gaining popularity as dielectric materials. Polymers are ideal candidates for many applications because they are easy to process, have tunable physical properties, are cost effective and can be manufactured according to specific needs. They also have excellent chemical resistance (“Dielectric Properties.”).

The dielectric constant of a material is a dimensionless parameter that describes its tendency to polarize in response to an applied electrical field. It is the ratio of the applied external field (E_0) to the electric field inside the dielectric material (E). The following equation is used to define the dielectric constant, ϵ :

$$\epsilon = E_0 / E \tag{2.1}$$

In the following section, the relationship between the refractive index, n , and the dielectric constant will be discussed.

2.2 Refractive index

The refractive index of a material is one of the most significant defining properties of an optical material. It is a measure of how the speed of light changes as it travels from a vacuum into a material. In the most simplified terms, the refractive index defines how much light is bent or “refracted” when crossing into different mediums. Overall, the refractive index, n , is defined as:

$$n = c/v \quad (2.2)$$

where,

c = velocity of light in a vacuum; v = velocity of light in the new medium

When light enters new medium from a vacuum, it decelerates due to the interaction of the electric and magnetic fields of light with the properties of the new material. As the speed of light is fastest in a vacuum, the refractive index of a vacuum is 1 and is thus used as the comparative standard against all other mediums (Dr. Rüdiger Paschotta).

According to Maxwell’s equations, the refractive index, n , of a non-magnetic material is dependent on the dielectric constant of the material:

$$n = (\epsilon)^{1/2} \quad (2.3)$$

where,

ϵ = dielectric constant of the material.

The refractive index is also dependent on many other factors. It can change due to the optical frequency or wavelength which is called chromatic dispersion. In general, the refractive index of glasses and crystals in the visible spectral region are within the range of 1.4 to 2.8. Usually, the refractive index increases for shorter wavelengths because the visible spectral region lies within the region of strong absorptance, the ultraviolet region lies within the region that has photon energies higher than the band gap energy and the near and mid-infrared region lies in a region with vibrational resonances and their overtones (Dr. Rüdiger Paschotta).

Temperature can also affect the refractive index and it usually has a direct proportional relationship with increasing temperature. Glass is an example to exceptions to this rule. Its refractive index decreases with increasing temperatures as the density of the material decreases. Other ways of modifying the refractive index include mechanical stresses and introduction of impurities, which is known as doping (Dr. Rüdiger Paschotta).

2.3 Dispersion and Absorption

The velocity of an electromagnetic wave through a solid in the simplest form is defined by the refractive index, n . The refractive index can be separated into two components, the real part n , which is related to the actual velocity and the complex part, k , known as the extinction coefficient, which is related to the decay or damping (absorption) of the oscillatory amplitude of the electric field as the wave propagates through matter. Therefore, the actual refractive index, $n^* = n - ik$, is dependent on how the electric field of the electromagnetic wave interacts with the matter it is traveling through.

Dielectric loss and non-zero DC conductivity in materials cause absorption. Good dielectric materials such as glass have extremely low DC conductivity, and at low frequencies, the dielectric loss is also negligible, resulting in almost no absorption ($\kappa \approx 0$). However, at higher frequencies (such as visible light), dielectric loss may increase absorption significantly, reducing the material's transparency to these frequencies (Mistrik et al. 2017).

The real and imaginary parts of the complex refractive index are related through use of the Kramers–Kronig relations. For example, one can determine a material's full complex refractive index as a function of wavelength from an absorption spectrum of the material.

2.4 Relation to dielectric constant

The dielectric constant (which is often dependent on wavelength) is simply the square of the (complex) refractive index in a non-magnetic medium (one with a relative magnetic permeability of unity). The refractive index is used for optics in Fresnel equations and Snell's law, while the dielectric constant is used in Maxwell's equations and electronics, where ϵ_1 , ϵ_2 , n , and κ are functions of wavelength:

$$\tilde{\epsilon} = \epsilon_1 + i\epsilon_2 = (n + i\kappa)^2 \quad (2.4)$$

Correlations between refractive index and dielectric constant is given by:

$$\epsilon_1 = n^2 - \kappa^2 \quad (2.5)$$

$$\epsilon_2 = 2n\kappa \quad (2.6)$$

$$n = \sqrt{\frac{\epsilon_1^2 + \epsilon_2^2 + \epsilon_1}{2}} \quad (2.7)$$

$$k = \sqrt{\frac{\epsilon_1^2 + \epsilon_2^2 - \epsilon_1}{2}} \quad (2.8)$$

2.5 Reflection

Reflectivity is defined as fraction of light reflected at an interface,

$$R = \frac{I_R}{I_0} \quad (2.9)$$

where I_0 and I_R are the incident and reflected beam intensities respectively.

If the material is in a vacuum or in air, then:

$$R = \left(\frac{n-1}{n+1}\right)^2 \quad (2.10)$$

The above equations apply to the reflection from a single surface and assume normal incidence. The value of R depends on the angle of incidence. Materials with a high index of refraction have a higher reflectivity than materials with a low index. Because the index of refraction varies with the wavelength of the photons, so does the reflectivity. In metals, the reflectivity is typically on the order of 0.90-0.95, whereas for glasses, it is close to 0.05. The high reflectivity of metals is one reason that they are opaque. High reflectivity

is desired in many applications including mirrors, coatings on glasses, etc. (Dr. Rüdiger Paschotta).

2.6 Absorption

When a light beam is impinged on a material surface, portion of the incident beam that is not reflected by the material is either absorbed or transmitted through the material. Bouguer's Law states that the fraction of beam that is absorbed is related to the thickness of the materials and the way the photons interact with the material's structure.

$$I = I_0 \exp(-\alpha x) \quad (2.11)$$

where,

I = intensity of the beam coming out of the material,

I_0 = intensity of the incident beam,

x = path through which the photons move, and

α = linear absorption coefficient, which is characteristic of the material.

Absorption occurs mainly by two mechanisms: Rayleigh scattering and Compton scattering. In Rayleigh scattering, the photon interacts with the electrons orbiting an atom and is deflected without any change in photon energy. This is significant for high atomic number atoms and low photon energies. In Compton scattering, interacting photon knocks out an electron losing some of its energy during the process. This is also significant for high atomic number atoms and low photon energies. Photoelectric effect occurs when photon energy is consumed to release an electron from the atomic nucleus. This effect

arises from the fact that the potential energy barrier for electrons is finite at the surface of the metal (Dr. Rüdiger Paschotta).

2.7 Transmission

Fraction of light beam that is not reflected or absorbed is transmitted through the material.

$$I_t = I_0(1 - R)^2 \exp(-\alpha x) \quad (2.12)$$

2.8 Emissivity

All objects at temperatures above absolute zero emit thermal radiation. However, for any particular wavelength and temperature, the amount of thermal radiation emitted depends on the emissivity of the object's surface (National Physics Laboratory).

Emissivity is defined as the ratio of the energy radiated from a material's surface to that radiated from a perfect emitter, known as a blackbody, at the same temperature and wavelength and under the same viewing conditions. It is a dimensionless number between 0 (for a perfect reflector) and 1 (for a perfect emitter). The emissivity of a surface depends not only on the material but also on the nature of the surface. For example, a clean and polished metal surface will have a low emissivity, whereas a roughened and oxidized metal surface will have a high emissivity. The emissivity also depends on the temperature of the surface as well as wavelength and angle (National Physics Laboratory).

Knowledge of surface emissivity is important both for accurate non-contact temperature measurement and for heat transfer calculations. Radiation thermometers detect the thermal radiation emitted by a surface. They are generally calibrated using blackbody reference sources that have an emissivity as close to 1. When viewing 'real', more

reflective surfaces, with a lower emissivity, less radiation will be received by the thermometer than from a blackbody at the same temperature and so the surface will appear colder than it is unless the thermometer reading is adjusted to take into account the material surface emissivity (National Physics Laboratory).

Unfortunately, because the emissivity of a material surface depends on many chemical and physical properties, it is often difficult to estimate. It must either be measured or modified in some way, for example by coating the surface with high emissivity black paint, to provide a known emissivity value.

2.9 Kramers-Kronig relations and the Cauchy method

There are a variety of applications in engineering where it is necessary to obtain information about a system over a broad range. However, in most cases, it is not possible to evaluate the parameter of interest in a closed form because either theoretical or experimental data is available over a narrow band. Generation of the data over the broad band is not possible or may be extremely time-consuming. A combination of Kramers-Kronig relations and the Cauchy method are often used to extrapolate/interpolate the data over a wide band (Krivokhvos 2014).

Kramers-Kronig (K-K) dispersion relations are one of the most important methods of analyzing light matter interaction phenomena in transparent matter, gases, molecules, and liquids. They provide restrictions for checking the self-consistency of experimental or model-generated data. Also K-K relations give the possibility for optical data inversion, i.e. information on dispersive phenomena can be obtained by converting measurements of absorptive phenomena over the whole spectrum and vice versa. These general properties

allow the framing of distinguishing phenomena that are very relevant at given frequencies showing that their dispersive and absorptive contributions are connected to all the other contributions in the rest of the spectrum. These properties relate to the principle of causality in light-matter interaction. Causality is one of the crucial principles in physics. The principle is derived from time order of cause and response of a system, i.e. the effect cannot precede the cause (Krivokhvos 2014).

The Cauchy method starts by assuming that the parameter of interest, as a function of frequency, can be approximated by a simple rational polynomial function. The method applied to the calculations in our simulations uses the singular value decomposition to evaluate the order of the polynomials and the coefficients that define them. Using this form, the parameter is evaluated at many frequency points (Adve et al. 1997).

CHAPTER 3

OPTICAL & ELECTRICAL PROPERTIES OF POLYMERS

Since the discovery of polymers, their exceptional dielectric characteristics have guaranteed their popularity of use as insulants in electrical and electronic engineering. In the nineteenth and early twentieth centuries, electrical apparatus mostly relied on wood, cotton sleeving, natural waxes and resins and later ebonite as insulating materials. Today, a variety of polymers including PTFE, PE, PVC, EP and MF provide an unparalleled combination of cost effectiveness, ease of processing and electrical performance. As these materials have developed, they have played a distinguished role in the evolution of electrical components and equipment. Since most electrical properties are determined largely by primary chemical structure and are relatively insensitive to microstructure, consequently, the electrical behavior of polymers is generally less disparate than its mechanical behavior. Similarly, optical properties also govern a variety of engineering end-uses (Hall 1981).

3.1 Behavior in a Steady (d.c.) Electric Field

The electrical properties of a material may be investigated by considering its response to imposed electric fields of various strengths and frequencies, just as the mechanical properties may be defined through the response to static and cyclic stress. We consider first the behavior of polymers in steady (d.c.) electric fields (Hall 1981).

Polymers as a class have the very high electrical resistivity characteristic of insulators. This implies that Ohm's law is obeyed and that the conduction current $I = AE/\rho$,

where E is the electric field strength, A is the cross-sectional area of the material and ρ is the resistivity. The volume resistivity measured by standard test methods increases steadily with time. Conduction in the surface layers of a polymer material is often sensitive to humidity and surface contamination. The surface resistivity is determined from the flow of current between two electrodes in contact with one surface of a thin specimen of polymer material (Hall 1981).

The extremely low values of current at typical working voltages implied by the high values of ρ show the absence in polymers of any large number of charge carriers such as in metals and semiconductors. The valence electrons in polymer molecules are localized in covalent bonds between pairs of atoms. The small current flow in weak fields arise from the movement of electrically charged species present as structural defects and impurities. To reduce the resistivity, the concentration of defects increases as the temperature rises. Exposure to ionizing radiation and absorption of water or plasticizer can also lead to an increase in the concentration of charge carriers with an additional increase in conductivity (Hall 1981).

In an ideal insulator, there is no steady current flow in a static electric field, but there is energy stored in the material as a result of dielectric polarization. The effect is similar to the storage of mechanical energy in a perfect elastic material, and formed through the displacement of electric charge. Some polarization occurs in all materials through small displacements of electrons and nuclei within individual atoms, but larger effects arise if the solid contains permanent dipoles (from polar bonds or asymmetric groups of atoms) which align in the direction of the external field. At normal electric field strengths, the dielectric polarization is proportional to the field strength, and we are able to define an important

linear property of the material, the relative permittivity (or dielectric constant), ϵ_r , which is the ratio ϵ/ϵ_0 of the permittivity of the material to the permittivity of a vacuum. The permittivity regulates the size of the force acting between a pair of electric charges separated by the dielectric material (Hall 1981).

The values of d.c. relative permittivities are determined by the nature and arrangement of the bonds in the primary structure. In polymers such as Polyethylene, Polypropylene and Polytetrafluoroethylene there is no dipole due to symmetry. Also, both bonding and non-bonding electrons are tightly held and slightly displaced by external fields. These materials exhibit very little dielectric polarization and result in a lower ϵ_r . However, polar polymers such as Poly(methyl methacrylate) (PMMA), Polyvinyl chloride (PVC) and Polyvinylidene fluoride (PVDF) have higher values of ϵ_r (Hall 1981).

The insulating property of any dielectric breaks down in strong electric fields. However, in polymers, the dielectric (or electric) strength may be as high as 1000 MV/m and an upper limit on dielectric strength is set by the ionization energies of electrons in covalent bonds within the primary structure of the polymer. Purely electrical or internal breakdown occurs when an adequate number of electrons are separated from their parent molecules and accelerate in the electric field to cause secondary ionization and avalanching. Even though the breakdown of this kind runs its course extremely rapidly, its voltage does not depend greatly on temperature (Hall 1981).

3.2 Optical Properties

There is a continuity present in the electrical and optical behavior of materials; for example, the optical refractive index n and the high frequency permittivity are linked in

electromagnetic theory. Absorption of optical radiation occurs by rearrangements of electrons within molecules (visible and ultraviolet) and excitation of bond vibrations (infrared). Additionally, scattering phenomena play a major role in determining optical properties. Light scattering is a display of optical diffraction processes, which takes place noticeably in polymer materials due to their having microstructural features of dimensions comparable with optical wavelengths (Hall 1981).

3.3 Color and Infrared Absorption

Only a few numbers of pure polymers absorb radiation in the visible spectrum, which is roughly between 380 and 760 nm, resulting in most polymers being colorless. The only few exceptions are some thermosets and elastomers, including Phenol formaldehyde resins (PF), some polyurethanes, epoxies and furan resins. They absorb strongly at the blue end of the spectrum and as a result, appear brownish when viewed by reflected light. These substances contain alternating double and single covalent bonds or aromatic rings which act as chromophores, absorbing light at frequencies corresponding to the excitation energies of bonding electrons. Polymer materials, that have been deliberately colored, are produced by incorporating as additives either finely divided colored solids (pigments) or soluble colored substances (dyes). The colors of solid polymers are fully defined by their spectra, measured either by transmission or reflection, whichever appears as more appropriate (Hall 1981).

Even though several polymers show no absorption of radiation at visible wavelengths, they are known to regularly absorb strongly at certain frequencies in the infrared. The infrared (transmission or reflectance) spectrum of a polymer is defined by its

molecular structure and infrared spectroscopy is one of the most powerful methods of polymer analysis, enabling polymer materials of unknown composition to be identified effortlessly from small samples (Hall 1981).

3.4 Refraction

Apart from color, the visual appearance and optical performance of a polymer material is dependent on the nature of its surface and its light transmission properties. When a ray of light strikes the plane surface of a colorless transparent material, the optical phenomena which takes place are governed by the refractive index n . Snell's law relates the angle r to the angle i ; Fresnel's equation allows the intensities and polarizations of the refracted and reflected rays to be calculated. n varies with wavelength and accurate determinations are made with monochromatic light, at specified wavelengths, using selected lines from the atomic emission spectra of elements (Hall 1981).

Refractive index is generated by the extent to which the electronic structure of the polymer molecules is deformed by the optical frequency of the incident electromagnetic radiation. If a material is structurally isotropic, which would be so in the case of unstressed amorphous polymers, then it is also optically isotropic, and a single refractive index typifies the refraction behavior. In crystals and other anisotropic materials, the refractive index takes different values along different principal axes, and the material is said to be doubly refracting or birefringent concluding in amorphous materials under deformation developing birefringence, as molecules become aligned. Similar effects arise in flowing polymer melts. As a result, the study of birefringence is an extensively useful method of exploring the microstructural effects of deformation. One particularly important technical

application of stress-induced birefringence in polymer materials is in photoelastic stress analysis. This is a method that explores complex stress distributions in engineering components and structures (Hall 1981).

3.5 Transparency

Polymeric materials that are colorless range from highly transparent to opaque and a loss of transparency arises from light scattering processes within the material. This in turn distorts and diminishes the transmitted image. When light is incident on a surface perpendicularly, a small fraction of the incident flux is reflected from the surface at the point of incidence. The ratio of reflected to transmitted flux is calculated by Fresnel's equation. At an air-polymer interface, with $n_2 = 1.5$, about 4 per cent of the incident flux is reflected. If the air is replaced by a transparent liquid possessing the same refractive index as the polymer, then the surface reflection is eliminated (Hall 1981).

If the material is non-absorbing, optically homogeneous and isotropic, then the transmitted ray is able to propagate without losing its intensity. In the case of real materials, the transmitted ray may lose some intensity as it travels forward due to the result of scattering from refractive index inhomogeneities within the material. Such scattering is similar to ray splitting which takes place at the surface and is repeated whenever the ray encounters an alteration of refractive index within the material (Hall 1981).

The outcome of scattering is to reduce the dissimilarity between light and dark components of the object viewed through the transparent polymer, and consequently to produce haze in the transmitted image.

In polymer materials, heterogeneity of refractive index can take place due to differences of density in amorphous and crystalline regions within the polymer itself, or from solid particles embodied as pigments or fillers, or from voids. The degree or intensity of scattering is strongly dependent on the variation of refractive index and additionally on the size of the heterogeneities. The most systemized scattering is seen when the scattering centers are comparable in dimensions with the wavelength of light. The scattering of light in pigmented polymer films has been studied diligently in connection with the optical properties of paints. Crystalline polymers are normally translucent or opaque unless (as in polymethylpentene) there is little to negligible difference in the refractive indices of crystalline and amorphous regions or (as in cellulose triacetate) that the spherulites are unusually small. It is readily possible to intensify the transparency of polymer materials by assisted nucleation or by high-speed cooling from the melt, both means of reducing the spherulite size. Additionally, stretching is also an effective way to increase transparency, since spherulites are transformed into oriented fibrils which scatter light inefficiently (Hall 1981).

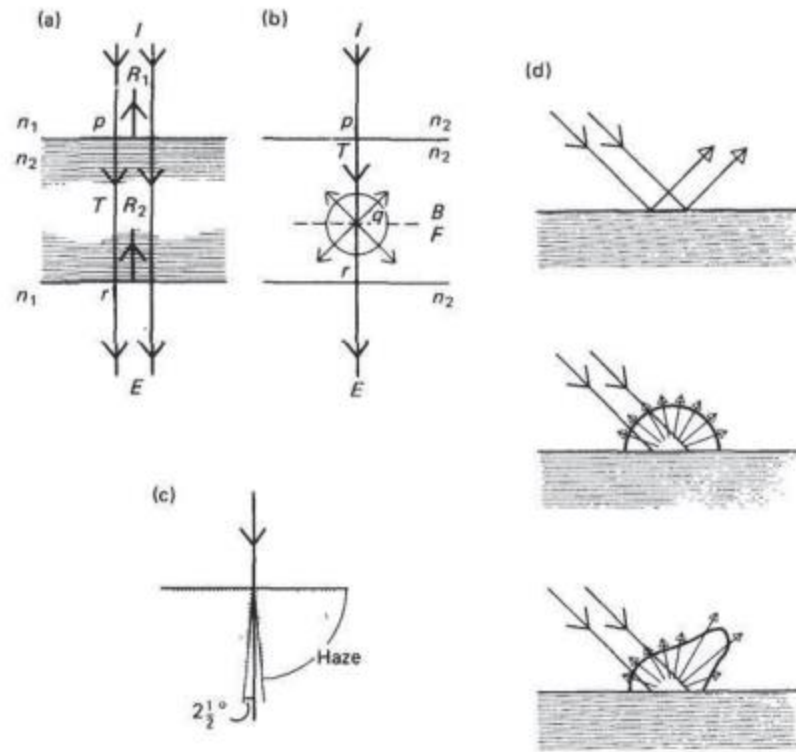


Figure 3.1 (a) Reflection and (b) scattering of light on transmission through a transparent medium, (c) Haze produced by wide-angle forward scattering of light, (d) Gloss: (from the top) specular reflection; perfect diffuse reflection; intermediate behavior. The polar envelope shows the angular distribution of reflected light intensity (Tran et al., 2016).

CHAPTER 4

FUNDAMENTALS OF DOPING OF POLYMERS

4.1 The Concept of Doping

Conducting polymers (CPs) have been doped using different methods in order to achieve high conductivities. Un-doped polymers are traditionally known as insulators but upon doping, their conductivity can change significantly and be comparable to metallic conductivity. Due to their unique chemical structures, however, the doping method for CPs is mechanistically different from that for their inorganic counterparts. Dopants in the polymer undergo redox reactions which causes charges to be transferred leading to the subsequent formation of charge carriers. The dopant withdraws electrons from the CP and also adds electrons to the CP backbone. Overall, electrons are extracted from the highest occupied molecular orbital (HOMO) of the valence band (oxidation) or transferred to the lowest unoccupied molecular orbital (LUMO) of the conduction band (reduction). This oxidation/reduction process creates charge carriers in the form of polarons, bipolarons, or solitons in the polymer (MacDiarmid, 1985).

CPs can be classified as degenerate and non-degenerate systems depending on their bond structures in the ground state. Degenerate polymers have two identical geometric structures in the ground state while non-degenerate polymers have two different structures with different energies in the ground state. Solitons are the charge carriers in degenerate systems such as polyacetylene and polarons and bipolarons are the charge carriers in both degenerate and non-degenerate systems such as Polypyrrole (PPy) and Polythiophene (PT). The movement of these charge carriers along polymer chains produces conductivity. The

oxidation and reduction processes in these reactions align with p-type and n-type doping, respectively (MacDiarmid, 1985).

In p-type doping, the electron moves directly from the HOMO of the polymer to the dopant species which creates a hole in the polymer backbone. In n-type doping, electrons from the dopant species move to the LUMO of the polymer creating an increased electron density. Thus, the density and mobility of charge carriers can be tuned by doping. The doping process generates positive or negative charge carriers which are delocalized over the polymer chains, thus facilitating electronic conductivity. Usually, the negatively charged carriers in n-doping are not as stable as positively charged carriers, which makes p-doping more popular in academic research as well as for practical applications (MacDiarmid, 1985).

4.2 Examples of the Effect of Doping on Optical Properties of Polymers

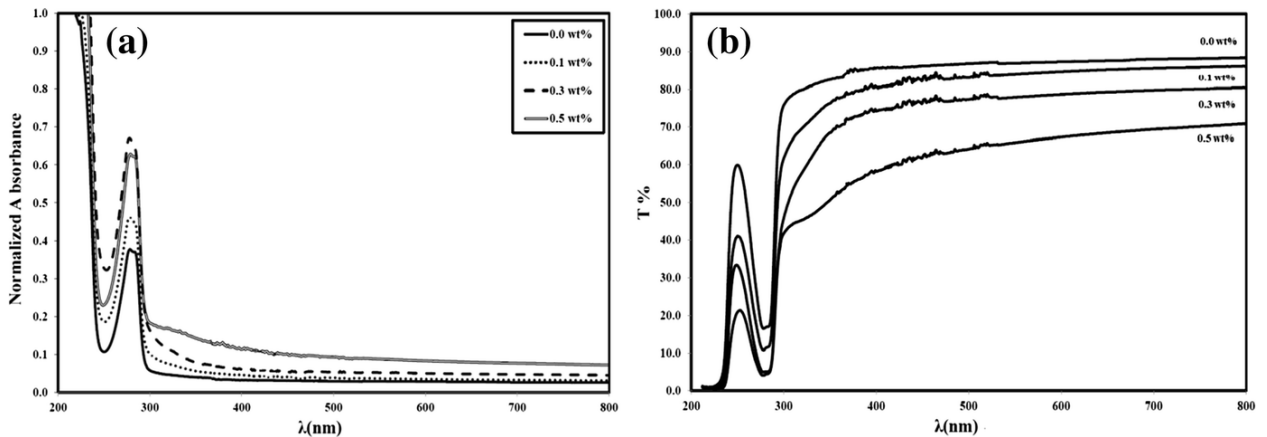


Fig 4.1 (a) Normalized absorbance of PVC/NiO nanocomposites films and (b) Transmittance spectra of these nanocomposites (Taha et al. 2018).

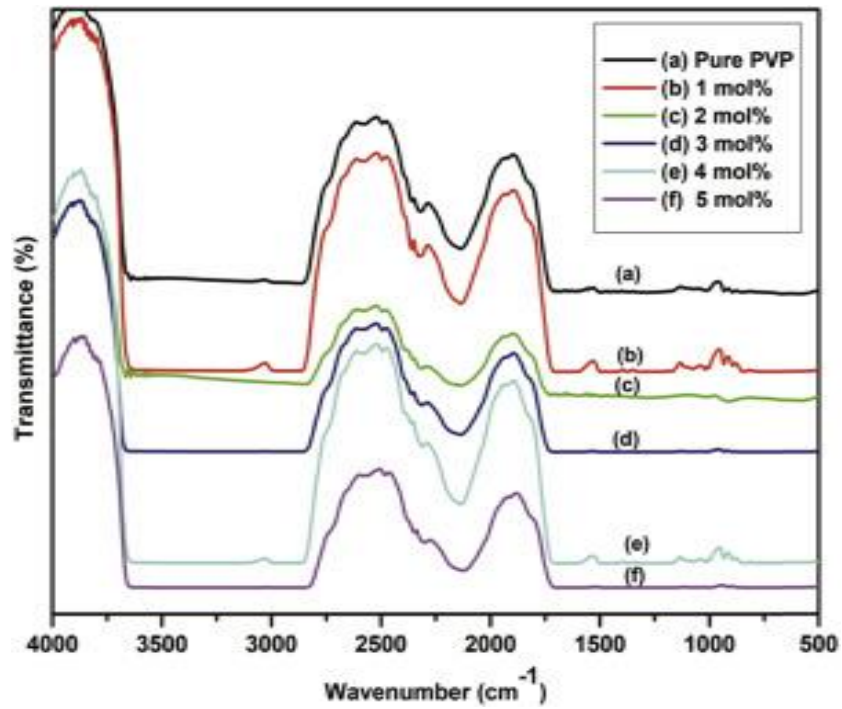


Figure 4.2 FTIR spectra of the pure and the VO²⁺ (1, 2, 3, 4, and 5 mol%) doped PVP polymer electrolyte films. (Sreekanth et al. 2019).

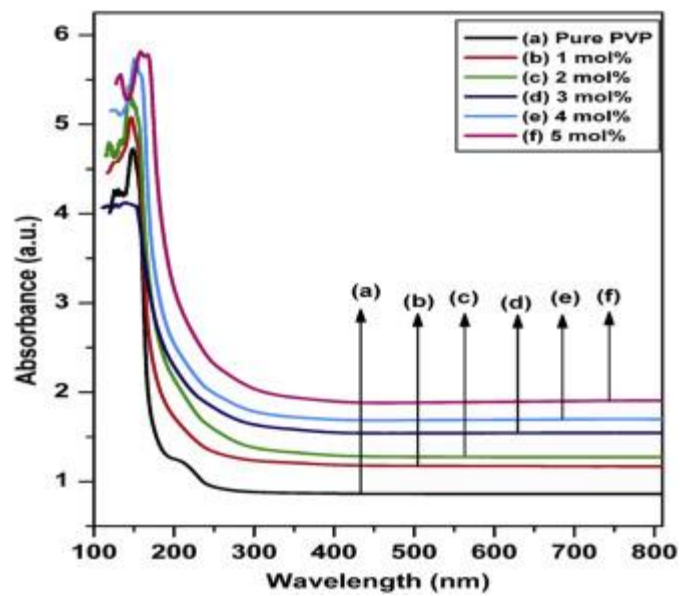


Fig 4.3 Absorbance spectra of the pure and the VO²⁺ (1, 2, 3, 4, and 5 mol%) doped PVP polymer electrolyte films (Sreekanth et al. 2019).

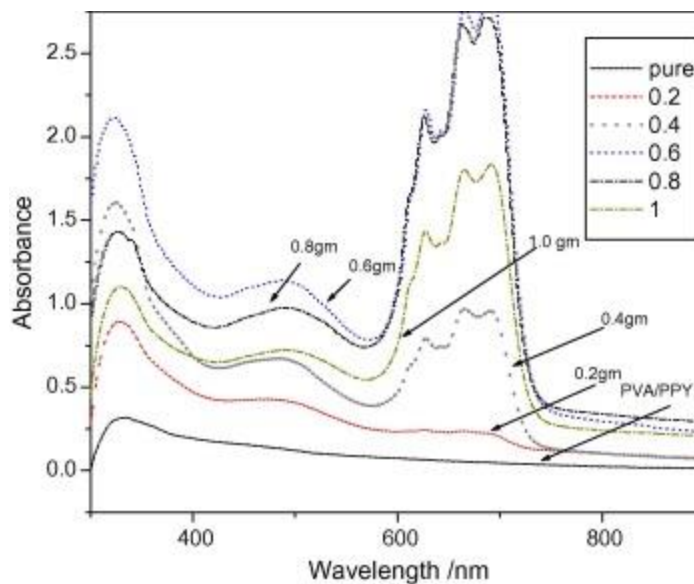


Figure 4.4 The absorbance spectra in the UV–VIS region for films of PVA/PPY and that doped with (0.2, 0.4, 0.6, 0.8 and 1.0 g of $\text{CoCl}_2 \cdot 6\text{H}_2\text{O}$) (Elkomy et al. 2016).

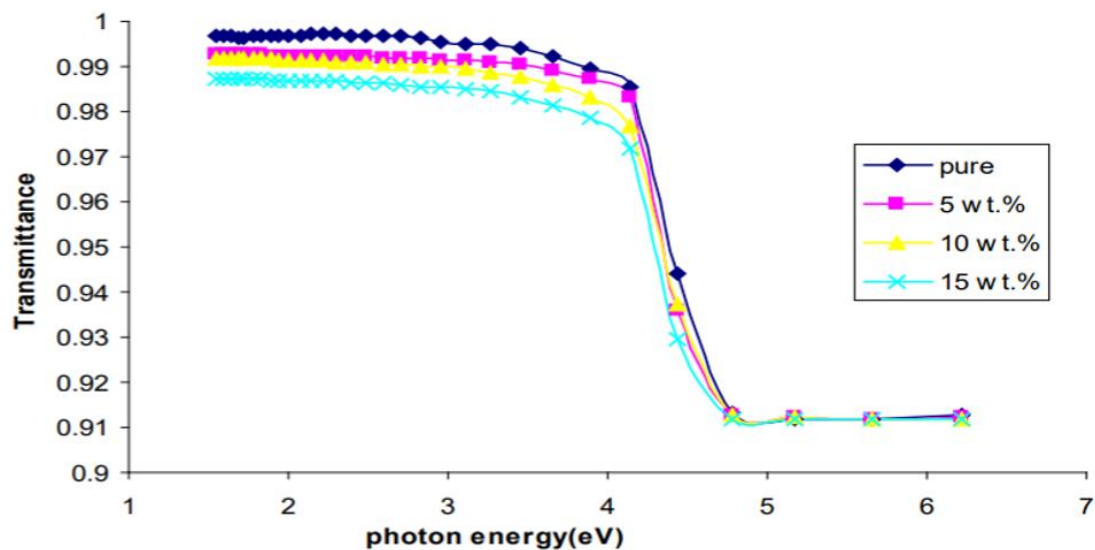


Figure 4.5 The variation of transmittance for (PVP-KBr) composite vs wavelength (Hakim et al. 2013).

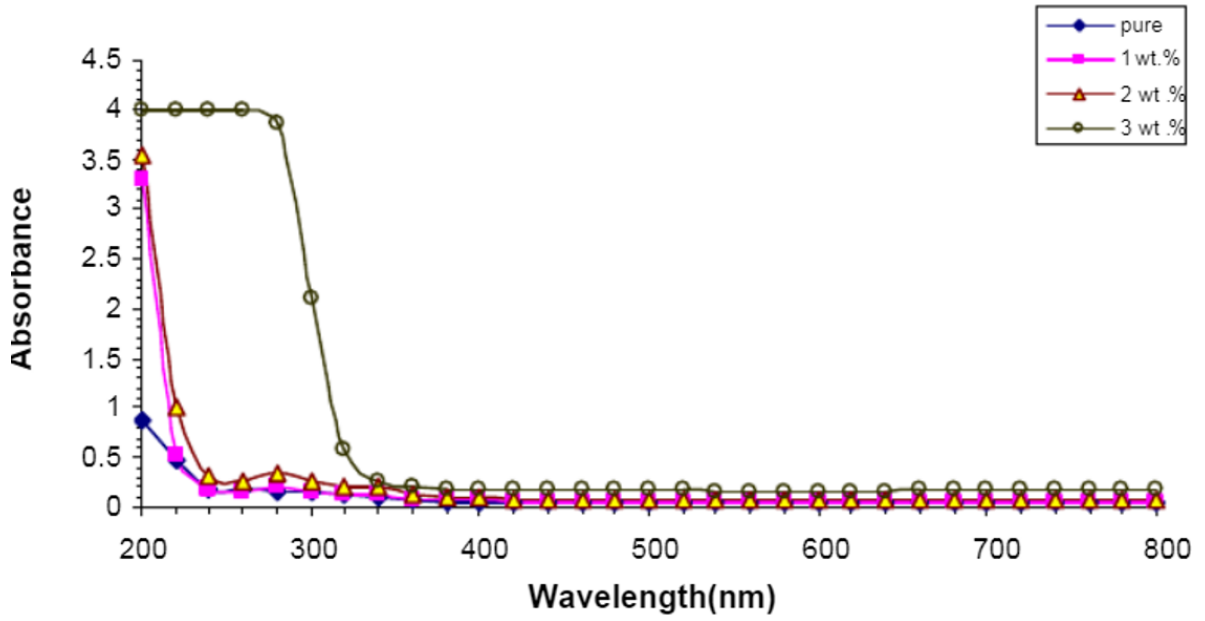


Figure 4.6 The variation of optical absorbance for (PVP-KBr) composite vs wavelength (Hakim et al. 2013).

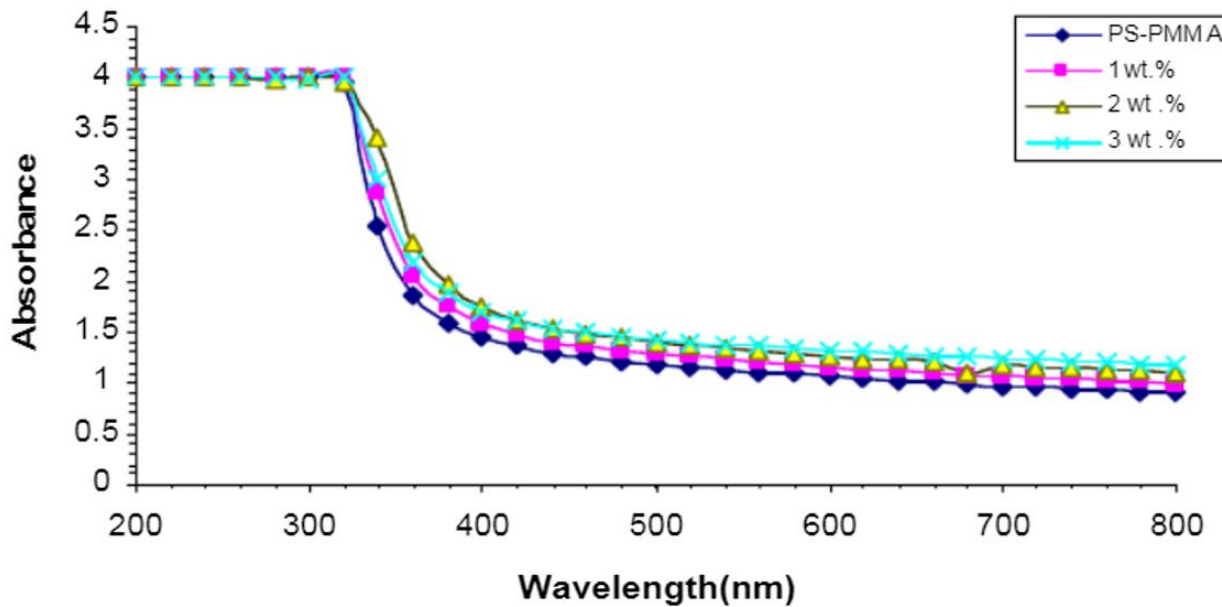


Figure 4.7 The variation of optical absorbance for PS-PMMA composite doped with NaF (Lafta et al, 2013).

4.3 Influence of Impurities on Optical Properties of Polymers

The introduction of impurities to polymers impact many of their properties, making them more applicable to various fields. It allows us to influence and tune certain characteristics, thus making them more advantageous to use. In this section, we will focus on the changes observed in the optical properties of polymers.

Many studies have been conducted on various combinations of polymers and impurities. Wasan Al-Taa'y et al. showed that PVC films doped with different nanosize zinc oxide (ZnO) concentrations affected various optical parameters such as extinction coefficient, refractive index, etc. The study concluded that the values for the extinction coefficient, refractive index, real and imaginary parts, infinitely high frequency dielectric constant, and average refractive index values had a positive correlation with the impurity percentage; i.e., they increased with increasing concentrations of ZnO. It was also noted that the optical conductivity increased with photon energy after doping.

Studies on PMMA embedded with gold nanoparticles showed that it had a strong influence on the imaginary part of the dielectric function with variation of size and weight fraction of the gold particles. Mixtures of PVA and Fe influence its absorption coefficient (Taha et al 2018). Such innumerable studies have been conducted on these exciting combination of materials and overall, an enhancement of desirable properties was observed with the introduction of impurities in polymers.

CHAPTER 5

WAVEGUIDE FUNDAMENTALS

Over the last decade, the continuous demand for greater speed and lower energy consumption in high bandwidth data links has driven the adoption of optical signaling in server backplanes due to the inherent limitations of copper technologies. As data rates continue to increase for consumer markets such as mobile communications, internet, and streaming media, data centers have increased their bandwidth capacities by a factor of 10 every 4 years. To increase this bandwidth, copper based signaling technologies are dominantly utilized with each technological node increasing in design complexity and cost (Swatowski, 2017).

Optical based technologies utilizing fiber optical connections are now being used more often to address the issues with electrical based signaling at higher data rates. However, these advances introduce manufacturing and density problems as fiber optical connections are not pre-routed connections like their electrical counterparts. The development of a method to route these optical connections in a cost-effective manner is required to continue growth of optical based signaling technologies (Swatowski, 2017).

Polymer waveguides serve as a potential candidate to enable high-density optical interconnections in data center architectures. Polymer waveguides typically are photopatternable materials that can be manufactured into complex optical routings on a small form factor. These materials can be manufactured onto flexible optical backplane or embedded into printed circuit boards. For polymer waveguides to become a realistic

technology for optical signal routing, manufacturing and stability requirements of the existing optical and printed circuit board industry must be maintained (Swatowski, 2017).

Dielectric waveguides are the structures that are used to confine and guide the light in guided-wave devices and circuits of integrated optics. A well-known dielectric waveguide is, of course, the optical fiber which usually has a circular cross-section. In contrast, the guides of interest to integrated optics are usually planar structures such as planar films or strips (Swatowski, 2017).

The simplest dielectric guide is the planar slab guide, where a planar film of refractive index n_f is sandwiched between a substrate and a cover material with lower refractive indices n_s and n_c ($n_f > n_s > n_c$). Often the cover material is air, in which case $n_c = 1$. Typical differences between the indices of the film and the substrate range from 10^{-3} to 10^{-1} , and a typical film thickness is $1 \mu\text{m}$. The light is confined by total internal reflection at the film-substrate and film-cover interfaces (Swatowski, 2017).

Assumptions made in this research are that the guided light is coherent and monochromatic and that the waveguides consist of dielectric media that are lossless and isotropic.

5.1 Optical Propagation

When light travels from a high index material into a low index material, a portion of the light is reflected and a portion is transmitted. The transmitted light enters the low RI medium at an angle that is calculated through the relationship in Equation 5.1 known as Snell's Law of Refraction.

$$n_1 \sin \theta_1 = n_2 \sin \theta_2 \quad (5.1)$$

When the angle of the high index material is large enough, the angle of refraction into the low index material is 90° as can be seen in Equation 5.2 and Figure 5.1. At this critical angle, all light is being reflected back into the high index material; so no light is being transmitted into the low index material. This is referred to as total internal reflection. This fundamental optical property of materials allows fiber optic propagation to occur.

$$\theta_1 \geq \sin^{-1} (n_2/n_1) \quad (5.2)$$

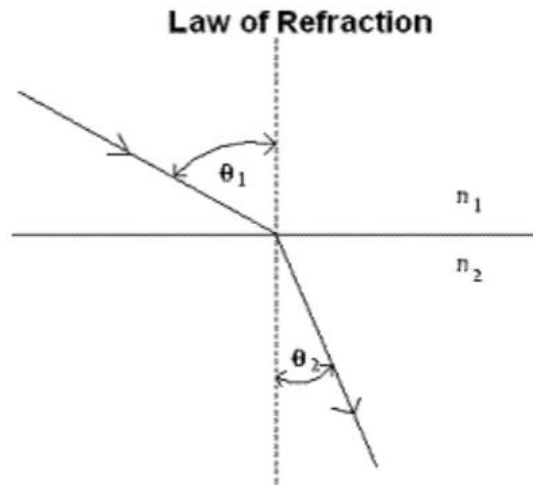


Figure 5.1 Snell's Law of Refraction.

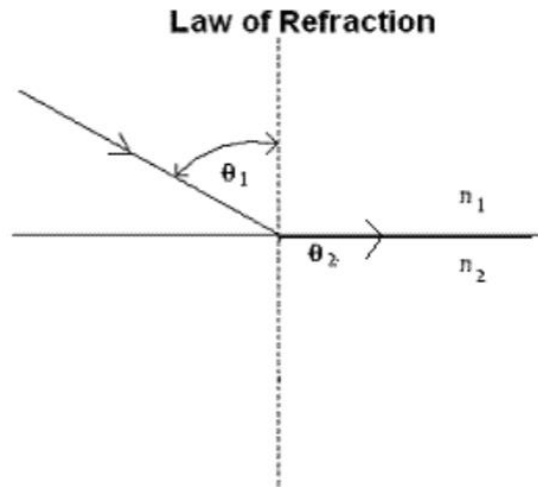


Figure 5.2 Total Internal Reflection (TIR).

Applying Snell's law of refraction between two interfaces and further extending it to a 2-dimensional rectangular slab with $n_1 > n_2$ (Figure 5.3), one can calculate the requirements of n_1 , n_2 , and θ_1 to restrict light to transmitting through a high index medium with no losses due to refraction. From Equation 5.3-5.5, θ_1 can be solved in terms of n_1 and n_2 . Equation 5.6 is the resulting relationship between the three variables and it can be seen that the angle of light entering a slab waveguide following the TIR principle is dependent on only the refractive indices of the two materials. This value is defined as the numerical aperture (NA) which is a measure of what angles of light are accepted into the waveguide and propagate without any refractive losses. When utilized in a wave guiding system, these materials are known as a core and clad where the core is the high RI region and the cladding is the low RI region.

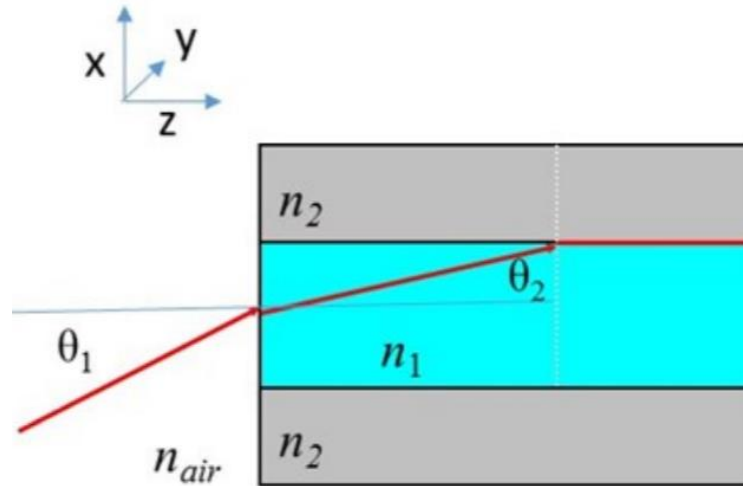


Figure 5.3 Slab Waveguide.

$$n_{air}\sin\theta_1 = n_1\sin\theta_2 \quad (5.3)$$

$$n_1\sin(90 - \theta_2) \geq n_2\sin 90 \quad (5.4)$$

$$\cos^2\theta_2 + \sin^2\theta_2 = 1 \quad (5.5)$$

$$NA \equiv \sin\theta_1 \leq \sqrt{(n_1^2 - n_2^2)} \quad (5.6)$$

Extending this optical phenomenon to 3 dimensions, Figure 5.4 depicts optical signaling being sent down a fiber optic cable. These optical fiber signals totally internally reflect, transmitting down the axis of a fiber optic to its destination. The level of the signal received is determined by two properties of the fiber optic, the attenuation and dispersion. Attenuation is the optical power loss of a fiber due to absorptions and scattering in the fiber. Dispersion is the amount that a signal will spread over a distance and is dependent on multiple factors such as fiber size, shape, NA, and others.

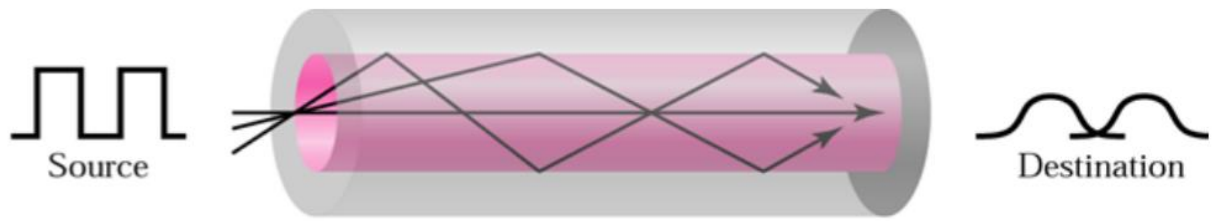


Figure 5.4 Fiber Optic Propagation.

Attenuation is defined as the exponential loss of light in a medium due to its intrinsic and extrinsic properties. For optical fibers and waveguides, the majority of attenuation is attributed to the material's molecular absorption of light and scattering due to impurities in the material or other optical phenomenon such as Rayleigh scattering. Attenuation is one of the primary factors in determining optical link lengths and viability in utilization of an optical channel (Swatowski, 2017).

Optical dispersion is a measure of the pulse broadening of a signal in an optical channel over a distance. This occurs due to multiple factors. First, light can travel down multiple paths while traveling down a fiber and this results in different total path lengths and pulse broadening. This is an example of modal dispersion and is dependent on device properties such as waveguide size and the refractive index difference between core and clad. For multimode fibers and waveguides, modal dispersion is the primary cause of dispersion. The other major cause of dispersion is chromatic dispersion; chromatic dispersion occurs because the speed of light in a medium is different for different wavelengths and since optical sources have a finite spectral output, the different wavelengths of light travel at different speeds. Chromatic dispersion is a major factor in the manufacture of single mode fibers where there is only one path for light and modal dispersion does not have an impact. For multimode links, chromatic dispersion has only a

small impact compared to modal dispersion and is typically ignored. Overall, dispersion plays an important role in optical communications especially over long distances (Swatowski 2017).

5.2 Boundary Conditions: Reflection and Transmission

When light is incident on a multilayer planar stack, it is reflected, refracted, and absorbed in a way that can be derived from the Fresnel equations. When the medium through which a wave travels suddenly changes, the wave often experiences partial transmission and partial reflection at the interface. Reflection is a wave phenomenon that changes the direction of a wavefront at an interface between two different media so that the wavefront returns into the medium from which it originated. Transmission permits the passage of wave, with some or none of the incident wave being absorbed. Reflection and transmission often occur at the same time ("Wave Behavior and Interaction | Boundless Physics").

As the signal propagates through the waveguide, it reflects internally multiple times at the interface. Each time this happens, we lose some of the signal due to partial transmission. The aim of this simulation is to predict how much loss occurs as the signal propagates through the waveguide.

We assume the structure to be a stack of one or more smooth planar layers and the interfaces between these layers are uniform and abrupt with no mixing. We also assume that the only attenuation faced by the signal is due to material properties and no other influences such as scattering. The thickness of the core is taken as 10 microns in diameter and the waveguide is assumed to be straight with no bending or twisting.

CHAPTER 6

SIMULATIONS

6.1 Description

In this study, the various waveguides were modeled using a semi-infinite plane containing three rectangular regions. All the regions run parallel to each other, with the top and bottom regions representing the cladding and the center region representing the core. The interfaces between each of the regions are assumed to be smooth. Each region is ascribed a value for \tilde{n} , the complex index of refraction. The values of \tilde{n} , as a function of wavelength, were extrapolated for each material. The simulation begins with a wave traveling from a vacuum entering the core region. The wave is described by the input parameters of wavelength, amplitude, phase, and polarization. As the wave travels through the core, it experiences attenuation caused due to absorption in the core region and losses at the core/cladding interface.

In order to account for the losses at the interfaces, all the coordinates where contact occurs are generated using the following relation:

$$(x_i, y_i) = (x_{i-1} + t/2 \tan \theta, 0) \text{ (if } i \text{ is even)} \quad (6.1)$$

$$(x_i, y_i) = (x_{i-1} + t/2 \tan \theta, t) \text{ (if } i \text{ is odd)} \quad (6.2)$$

The initial conditions for this relation are $(0, t/2)$ for $i = 0$ and $(t/2 \tan \theta, t)$ for $i = 1$. The variables t and θ represent the thickness of the core layer and the wave's angle of entry

respectively. After the contact coordinates are generated, the incoming electric field and outgoing electric field are generated using the relation:

$$E_i = r * E_{i-1} \quad (6.3)$$

where,

r = Fresnel reflectance coefficient.

The reflectance coefficient is given by:

$$r = (\tilde{n}_i \cos \theta_i - \tilde{n}_o \cos \theta_o) / (\tilde{n}_i \cos \theta_i + \tilde{n}_o \cos \theta_o) \quad (6.4)$$

(for transverse-magnet (TM) polarization)

$$r = (\tilde{n}_o \cos \theta_i - \tilde{n}_i \cos \theta_o) / (\tilde{n}_i \cos \theta_i + \tilde{n}_o \cos \theta_o) \quad (6.5)$$

(transverse-electric (TE) polarization)

After iterating through all the contact points, the final resulting electric field takes into account all the losses at the boundaries of the waveguide.

To account for the losses due to the absorption of the core material, the imaginary portion of the index of refraction is used. The equation:

$$E_{final} = E_{initial} \exp(\text{distance traveled} * 4\pi / \lambda) \quad (6.6)$$

gives the final electric field with absorption losses considered. Using both the absorption and boundary losses, the final electric field and intensity are calculated. To calculate the final attenuation, A , of the waveguide, the following equation was used:

$$A = 10\log_{10} [(Input\ Intensity) / (Output\ Intensity)] \quad (6.7)$$

To compare each of the various waveguide setups, various values for wavelength and length of the fiber were used to simulate the resulting attenuation losses.

Chapter 7

RESULTS & DISCUSSION

7.1 Poly(9,9-dioctylfluorene-alt-benzothiadiazole) (F8BT)

Conducting polymers (CPs) have been studied extensively in recent years because they exhibit remarkable electroluminescent and semiconducting properties that can be applied to a vast array of applications like organic light-emitting diodes, organic field-effect transistors, organic solar cells, and memory devices, among others. CPs also have the advantage of being compatible with a significant number of organic and inorganic materials which make it possible to create mechanically flexible substrates and thus be used over stretchable and bendable systems. They are also easy to process into partially transparent thin films and have low thresholds for Amplified Spontaneous Emission (ASE) which make them ideal for fabricating low-loss waveguides.

Through literature review, it was found that highly fluorescent conjugated polymer F8BT as the optical gain medium and a mechanically flexible and biodegradable CA polymer as a substrate, are a promising all-polymer waveguide system (Smirnov et al. 2016). The 2016 study conducted by Smirnov et al. used F8BT as the core material and Cellulose Acetate as the clad (CAISWG) to elevate refractive index contrast and thus enhance light confinement and optical amplification of the waveguides. The study also investigated Quartz/F8BT (QISWG) infinite slab waveguides as well as CA/F8BT asymmetrical ridge waveguides (ARWG), but it is beyond the means of the code to simulate the results for these two systems (Smirnov et al. 2016).

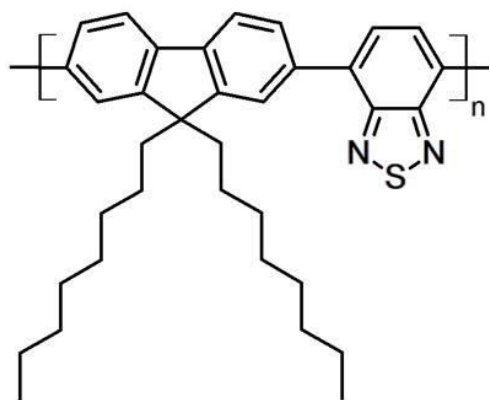


Figure 7.1 Chemical Structure of F8BT.

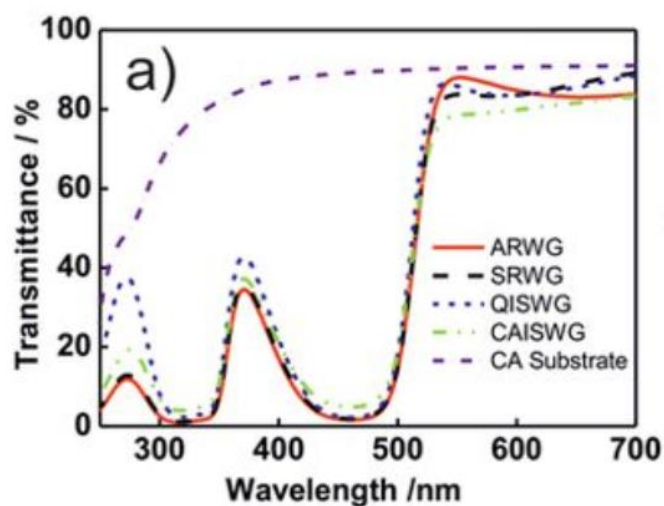


Figure 7.2: Transmittance spectra of CAISWG (green dash dot dot line), QISWG (blue short dash), ARWG (red solid line), SRWG (black dash line) and the used CA substrate (purple short dash dot) (Smirnov et al. 2016).

In our simulations, we took F8BT as the core and cellulose acetate as the cladding. The results obtained are comparable to the data provided in the study. We investigated a larger range into the near-IR and mid-IR region; in particular, three wavelengths, 850, 1300 and 1550 nm were of interest. We chose these specific prime wavelengths because NIST (the US National Institute of Standards and Technology) provides power meter calibration

at these three wavelengths for fiber optics; thus, they drive everything that is designed or tested for long- or short-range communications. Arbitrary lengths of 0.85, 1.30 and 1.55 m were chosen to demonstrate the relationship between signal attenuation and distance travelled. A schematic of the proposed system is shown below.

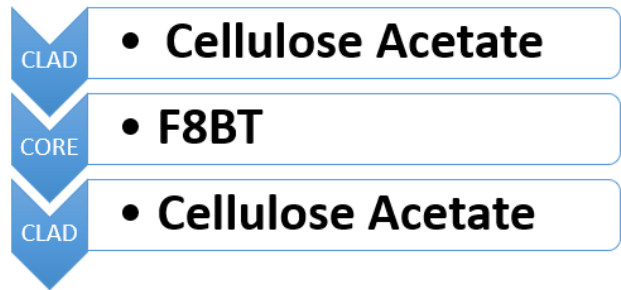


Figure 7.3 Schematic of proposed system with F8BT as core and Cellulose Acetate as clad

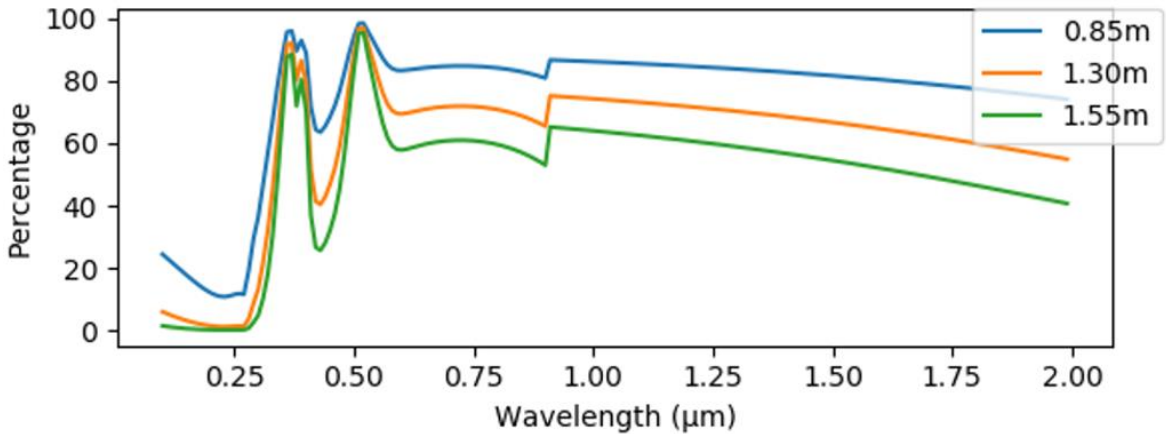


Figure 7.4 Simulated Transmittance spectra of Pure F8BT waveguide and Cellulose Acetate cladding.

We can observe comparable peaks and troughs at approximately 300, 400, 450 and 600 nm between the simulated spectra and the data obtained from the literature. Further, simulations were also performed using various combinations of F8BT, SiO₂ and Air to

show the changes in the signal with the chosen material. They are demonstrated in Figure 7.5.

We observe that the transmission spectra of F8BT core with CA clad has the most consistent transmission efficiencies over all lengths. As the length increases, the percentage of transmitted signal decreases and the higher the wavelength, the higher is the percentage loss in the signal. For other combinations, we observed that as expected, the shortest length always produced the least attenuation of the signal. The data is summarized in Table 7.1.

Table 7.1 F8BT Max and Min Values of its Transmission Spectra

	Clad: F8BT, Core: Air		Clad: CA, Core: F8BT		Clad: F8BT, Core: SiO ₂		Clad: SiO ₂ , Core: F8BT	
nm	T max	T min	T max	T min	T max	T min	T max	T min
850	35% @0.85m	0% @1.55m	85% @0.85m	55% @1.55m	70% @0.85m	10% @1.55m	50% @0.85m	4% @1.55m
1300	33% @0.85m	0% @1.55m	82% @0.85m	58% @1.55m	80% @0.85m	20% @1.55m	55% @0.85m	8% @1.55m
1550	30% @0.85m	0% @1.55m	80% @0.85m	55% @1.55m	87% @0.85m	30% @1.55m	59% @1.55m	10% @1.55m

The troughs and peaks are observed at analogous wavelengths for all combinations. The differences in the overall spectra can be attributed to the fact that we used different materials which changed the intrinsic properties of the waveguide. An interesting observation from the results of SiO₂ is that it can be used as cladding or core in combination with F8BT. This is because their refractive indices are not significantly different which is

why this phenomenon can occur; however, it is of academic interest as significant differences in n values are required for the waveguide to be efficient in real applications.

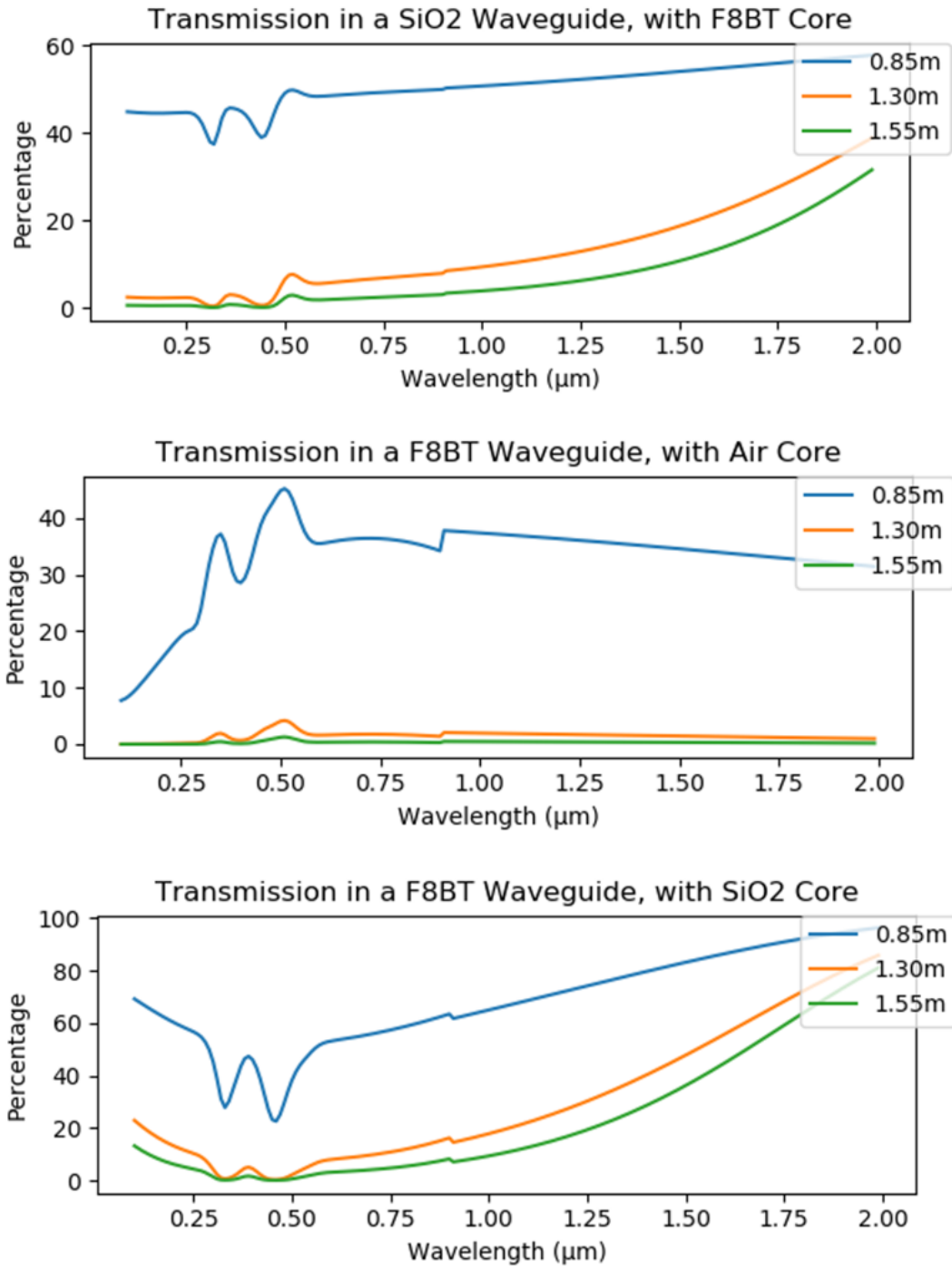


Figure 7.5 Simulated transmission spectra of F8BT waveguide system with a variety of materials as clad and core.

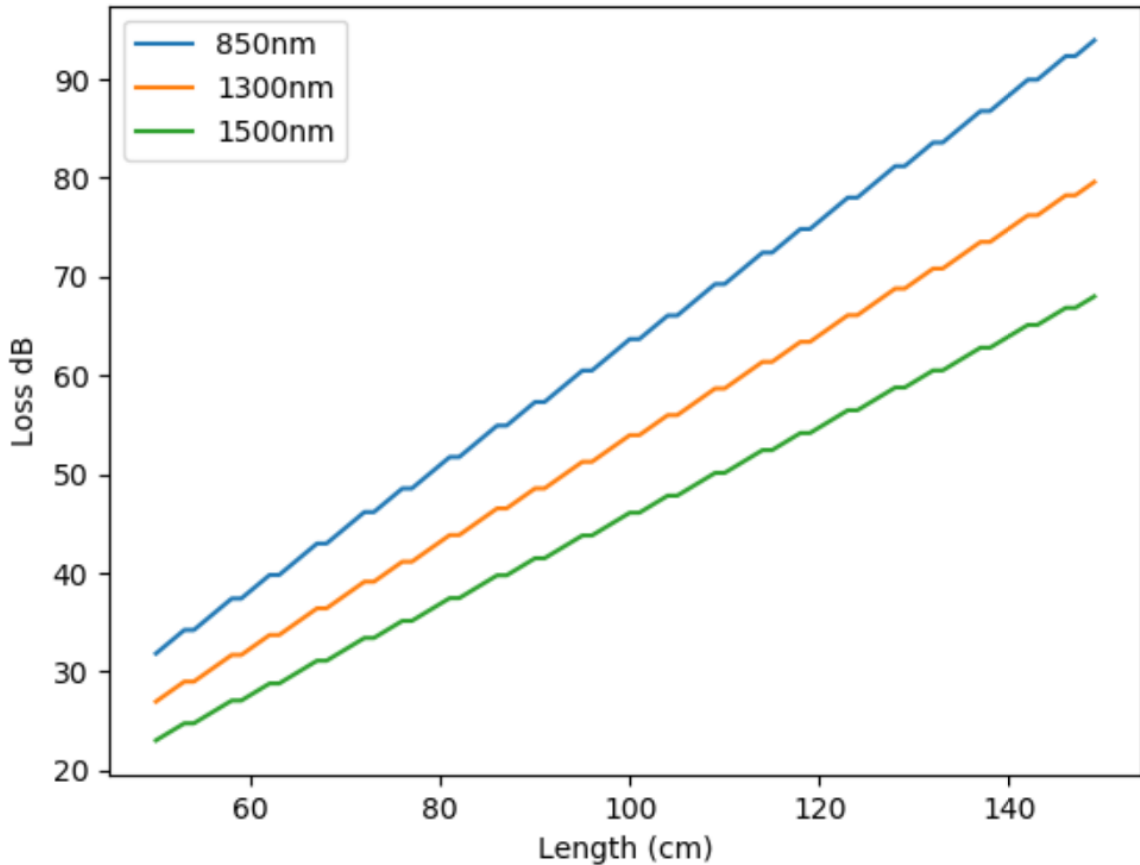


Figure 7.6 Signal loss of NIST suggested wavelengths in IR-range in F8BT waveguide (core) with Cellulose Acetate clad vs length (distance travelled).

From Figure 7.6, we can deduce that signal loss across the length of the waveguide is linear and is independent of the wavelength of the signal. However, shorter wavelengths attenuate significantly more than longer wavelengths.

7.2 Poly(methyl methacrylate) (PMMA)

Poly(methyl methacrylate) (PMMA) is one of the most favored materials used in optical applications because of its high transmission in the visible and near-infrared regions and its mechanical flexibility. It is used generally to fabricate plastic optical fibers and planar

waveguide devices. Figure 6.5 shows the chemical structure of the repeating monomer of PMMA.

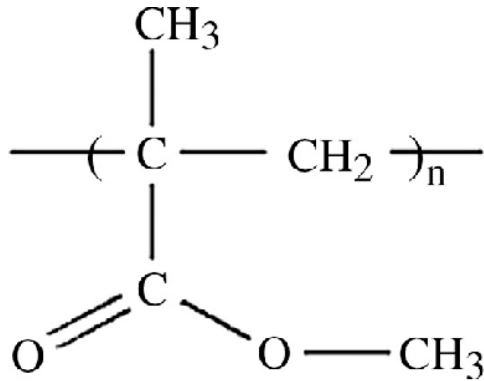


Figure 7.7 Chemical structure of PMMA.

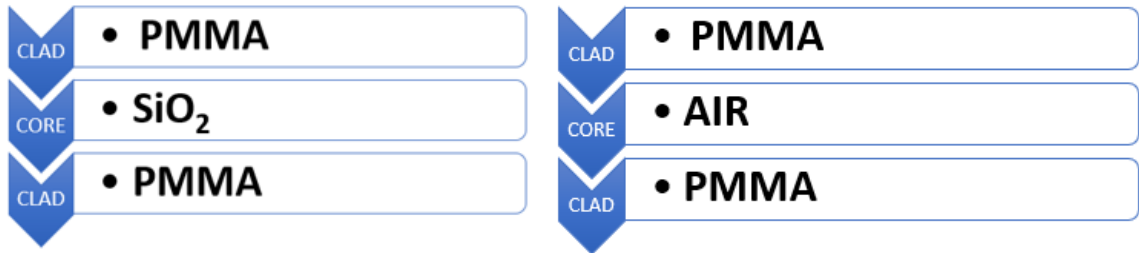


Figure 7.8 Schematic of the proposed waveguide systems involving PMMA.

In this study, we used PMMA as the cladding and air and SiO₂ as core for qualitative analysis. The results are shown in Figure 7.7 and summarized in Table 7.2.

In the first proposed waveguide system with PMMA as cladding and SiO₂ as core, we observe that for longer distances travelled, the signal loss is significant but at the shortest (considered) length of 0.85 m, the results are better with almost 60% transmission at higher wavelengths. There is a significant drop in transmission at about 300 nm for 0.85

m length. The longer waveguides have very low efficiencies and will probably not be relevant in real world applications. In the second system, with PMMA as clad and air as core, we observe significantly increased efficiencies of signal transmission especially at higher wavelengths but larger attenuation of the signal with increasing distance.

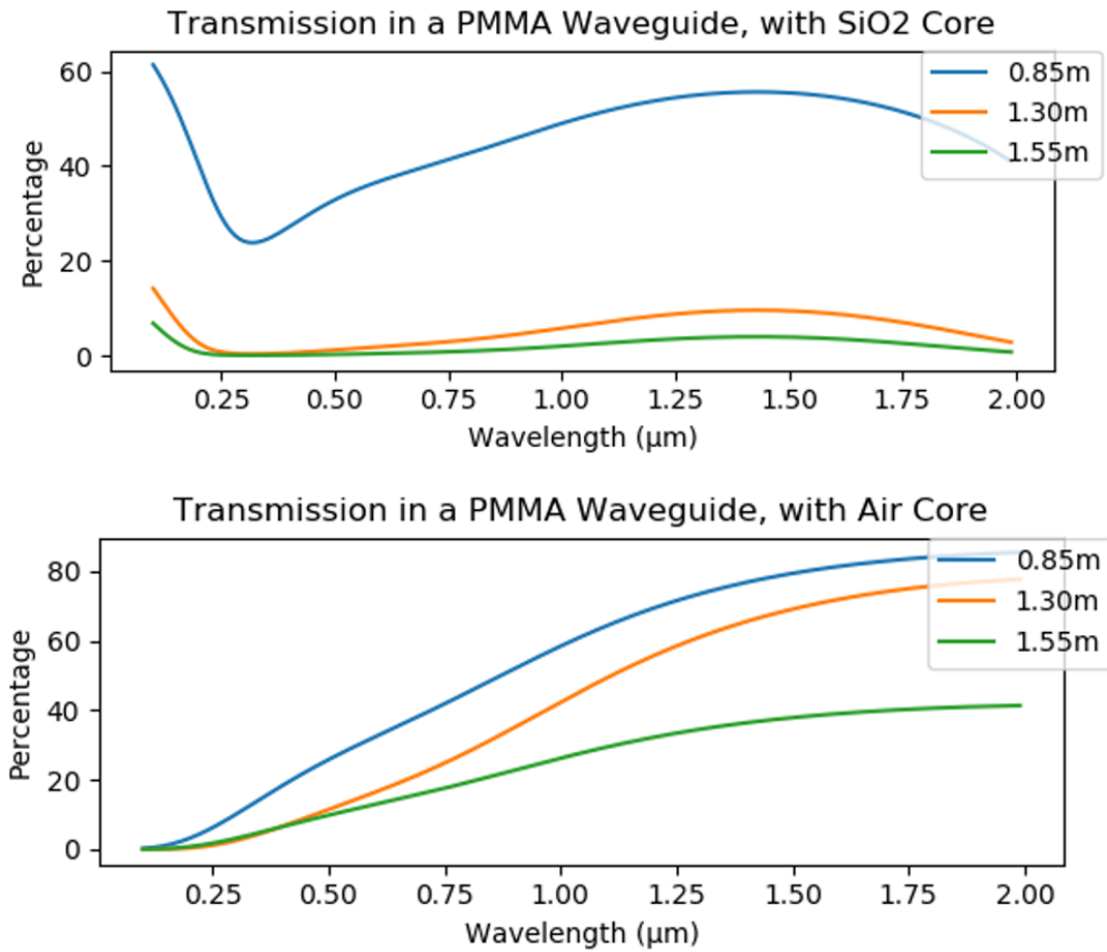


Figure 7.9 Simulated transmission spectra of PMMA waveguide as cladding and Air and SiO₂ as core.

Table 7.2 PMMA Waveguide Max and Min Values of its Transmission Spectra

	Clad: PMMA, Core: Air		Clad: PMMA, Core: SiO ₂	
nm	T max	T min	T max	T min
850	55% @0.85m	20% @1.55m	45% @0.85m	0% @1.55m
1300	75% @0.85m	30% @1.55m	58% @0.85m	5% @1.55m
1550	80% @0.85m	35% @1.55m	56% @0.85m	5% @1.55m

From the simulated results, we observe that the signal loss is linear and is independent of the wavelength in both systems. However, at larger wavelengths, the attenuation of signal is low over distance/length of the waveguide.

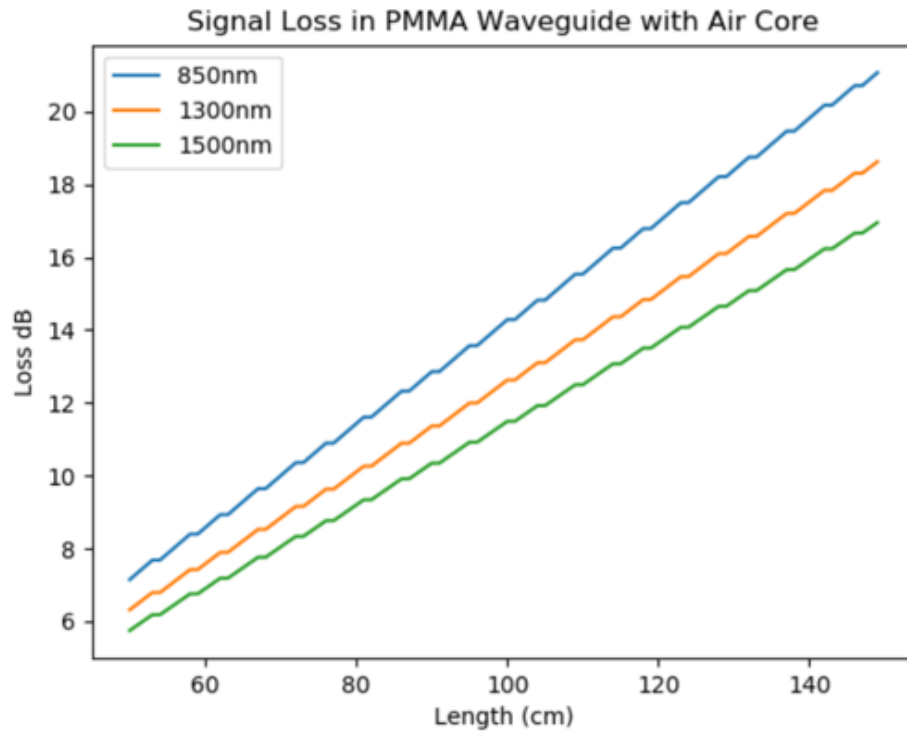
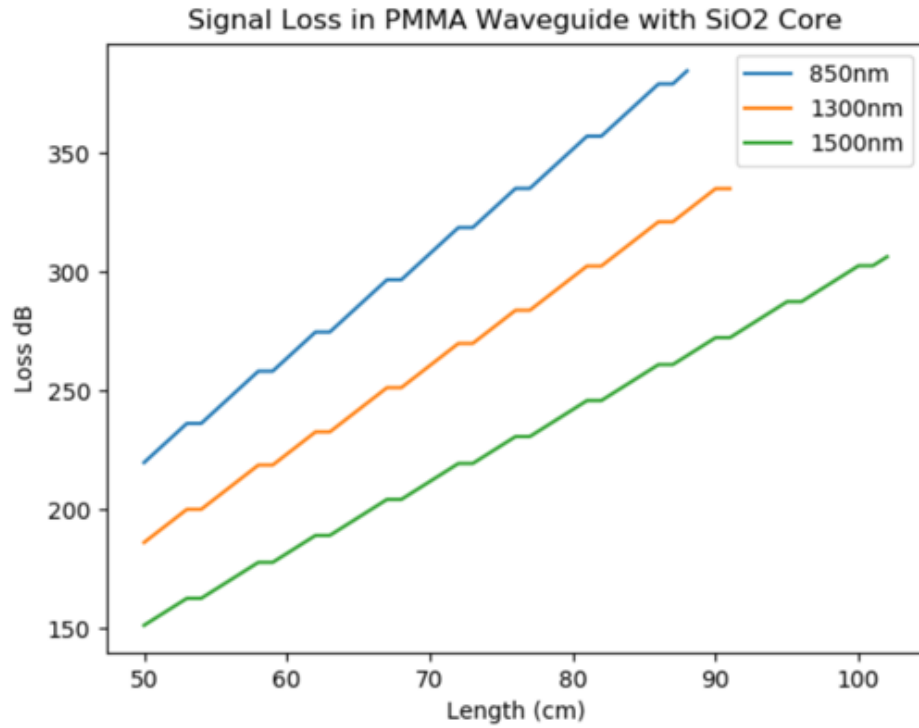


Figure 7.10 Signal loss of NIST suggested wavelengths in IR- range in waveguides with PMMA and SiO₂/Air systems vs length (distance travelled).

7.3 Poly(vinyl alcohol) (PVA)

Poly(vinyl alcohol) (PVA) is often used as an optical polymer but usually as composite with other materials to enhance its properties.

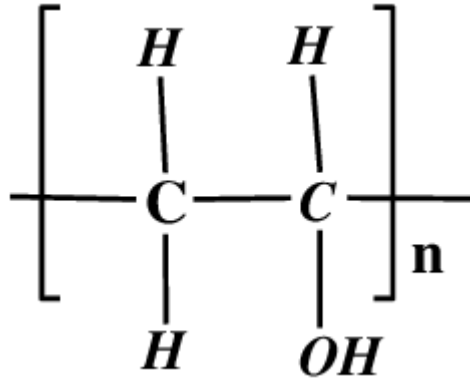


Figure 7.11 Chemical structure of PVA.

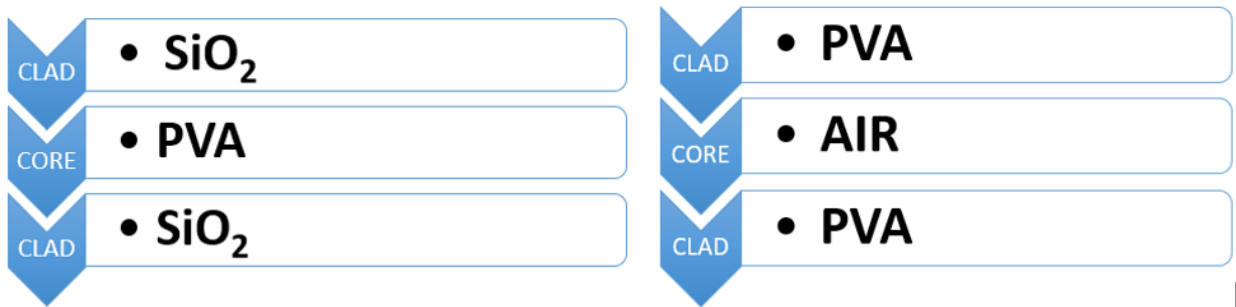


Figure 7.12 Schematic of proposed waveguide systems involving PVA.

In this study, two systems were proposed involving PVA. The first one is a polymer waveguide with a PVA core and SiO₂ clad and the second one is an air core with a PVA clad. The results obtained are shown in Figure 7.13 and summarized in Table 6.3.

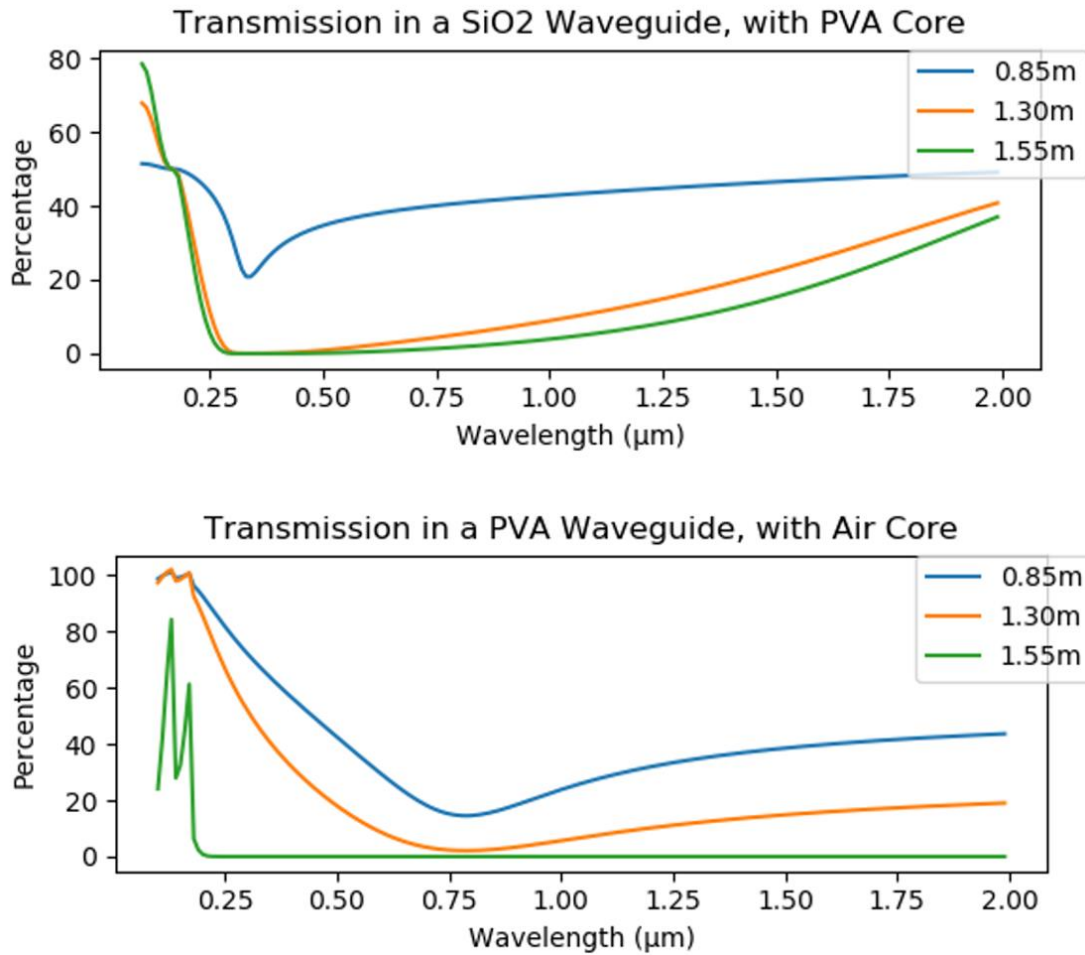


Figure 7.13 Simulated transmission spectra of PVA waveguide as core and SiO₂ as clad and Air as core and PVA as clad.

Table 7.3 PVA Waveguide Max and Min Values of its Transmission Spectra

nm	Clad: PVA, Core: Air		Clad: SiO ₂ , Core: PVA	
	T max	T min	T max	T min
850	30% @0.85m	0% @1.55m	45% @0.85m	3% @1.55m
1300	42% @0.85m	0% @1.55m	47% @0.85m	5% @1.55m
1550	40% @0.85m	0% @1.55m	47% @0.85m	17% @1.55m

In the first proposed waveguide system with PVA as core and SiO₂ as cladding, we observe that for longer distances travelled, the signal loss is significant but at the shortest length of 0.85 m, the results are better with almost 60% transmission at higher wavelengths. There is a significant drop in transmission at about 300 nm for 0.85 m length. The longer waveguides have very low efficiencies in the short wavelength range but increase to about 40% at the larger wavelengths. In the second system, with PVA as clad and air as core, we observe lower efficiencies and a significant drop at about 750 nm and then a gradual increase to about 40% and 20% for 0.85 m and 1.30 m respectively.

From analyzing the signal loss data, we conclude that the loss is linear and is independent of wavelength in both systems and at longer wavelengths, the waveguides exhibit lower rates of attenuation than shorter wavelengths.

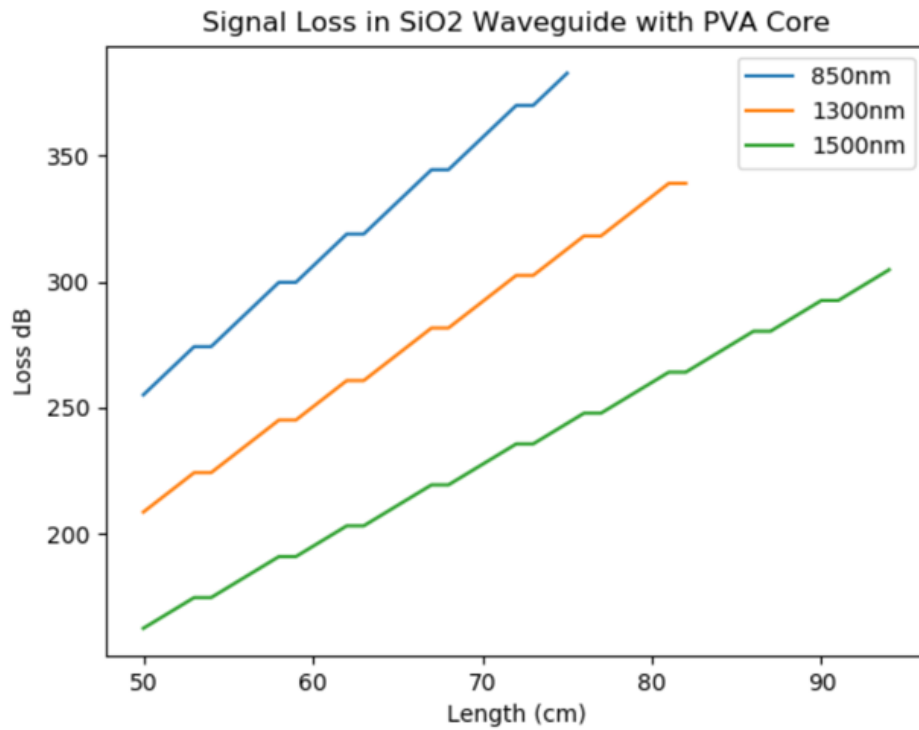
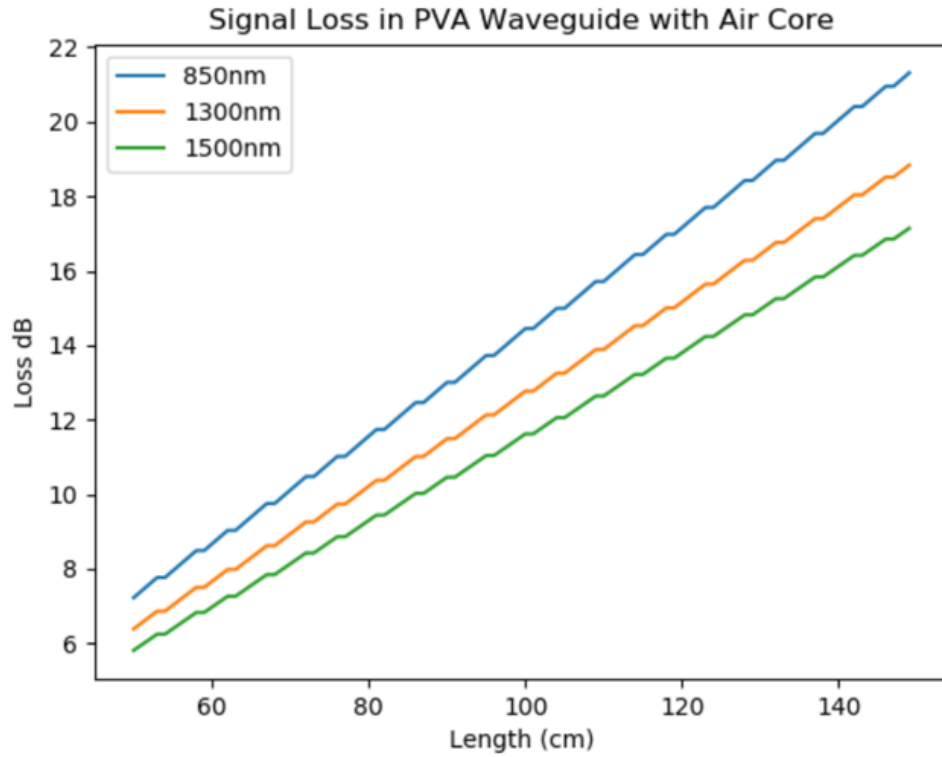


Figure 7.14 Signal loss of NIST suggested wavelengths in IR- range in waveguides with PVA and SiO₂/Air systems vs length (distance travelled).

7.4 Polyaniline (PANI)

Polyaniline (PANI) is a highly conductive polymer with attractive qualities such as low density, mechanical flexibility, easy processability and synthesis, tunable shielding response and high environmental stability. Thus, it can be seen as a competitor to metallic and semiconducting materials. PANI has many potential applications in a variety of technological functions such as rechargeable batteries, sensors, electronic devices, light-emitting diodes, conducting paints and glues, gas-separation membranes, coatings etc.

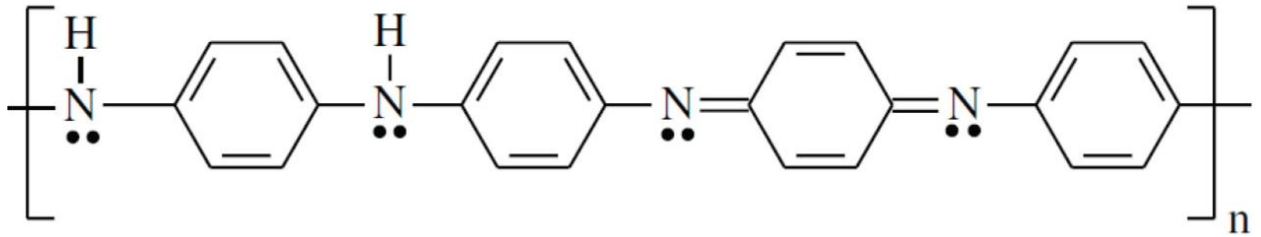


Figure 7.15 Molecular structure of the repeating unit for PANI-B.

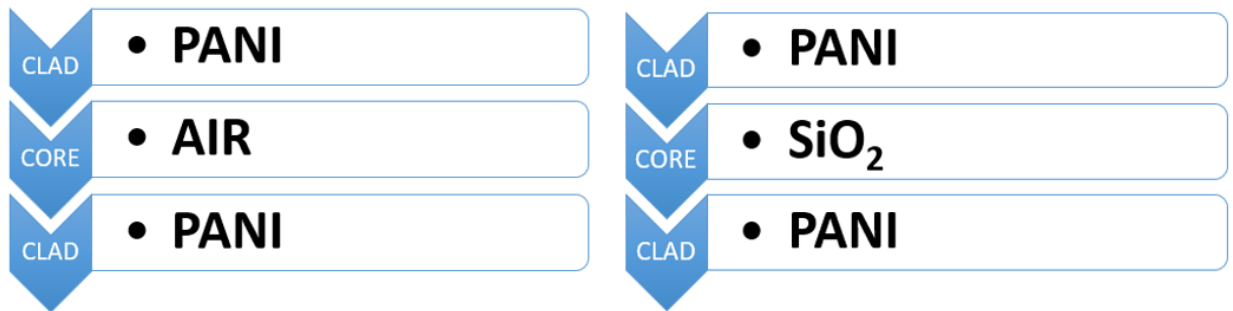


Figure 7.16 Schematic of proposed waveguide systems involving PANI.

There are no literature reviews of waveguides for the proposed systems and thus we cannot compare them with experimental data. However, after analyzing the simulated data, we can deduce that neither of the systems are very efficient. In the PANI clad and SiO₂ core system, we see a sharp decline in transmission in the UV region around 200 nm,

followed by a slight increase around 250 nm for all lengths. At higher wavelengths, the transmission efficiency decreases further and does not exceed 10% which suggests that this system might not have many real world applications in the form of waveguides. For the second system with an air core and PANI clad, all lengths show similar trends in the attenuation of the signal with the shortest length being most efficient and the longest being least efficient.

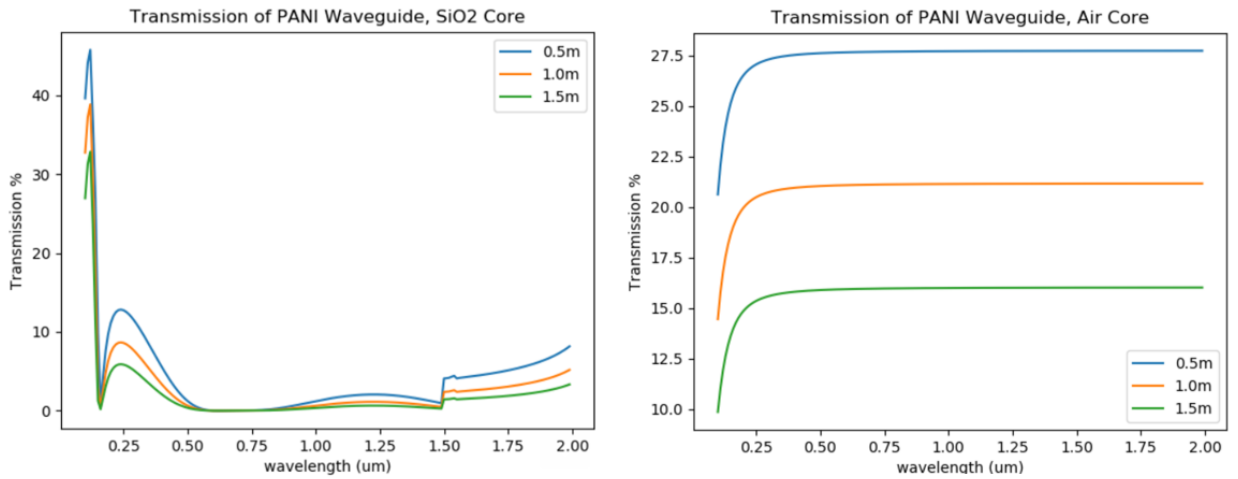


Figure 7.17 Simulated transmission spectra of PANI waveguide as clad and SiO₂ and Air as core.

Signal loss is linear and is independent of the wavelength in both systems and at longer wavelengths, the waveguides exhibit lower rates of attenuation than shorter wavelengths.

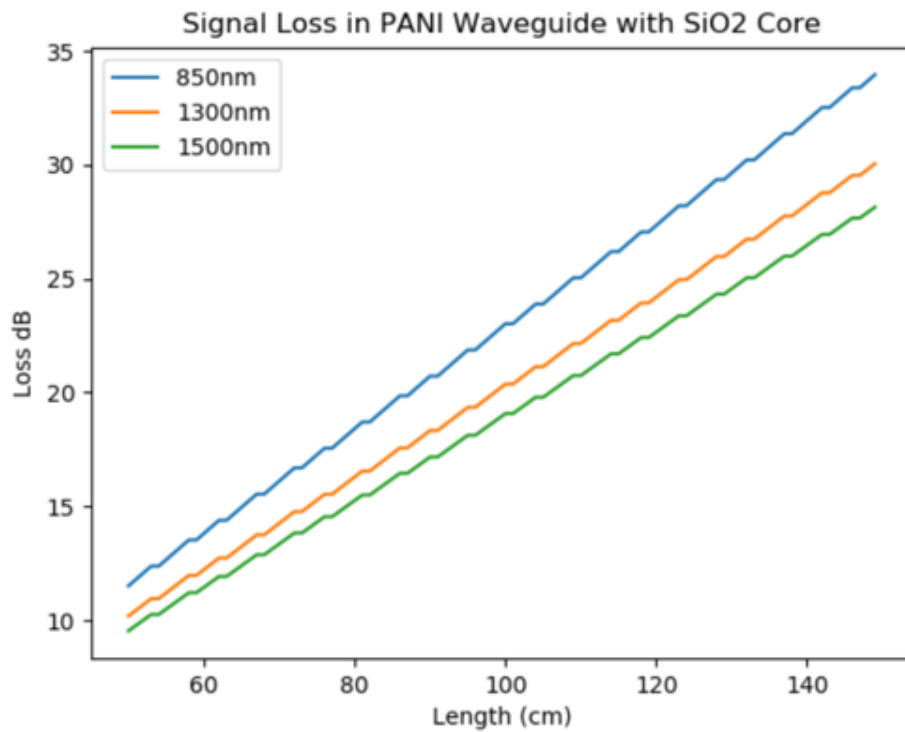
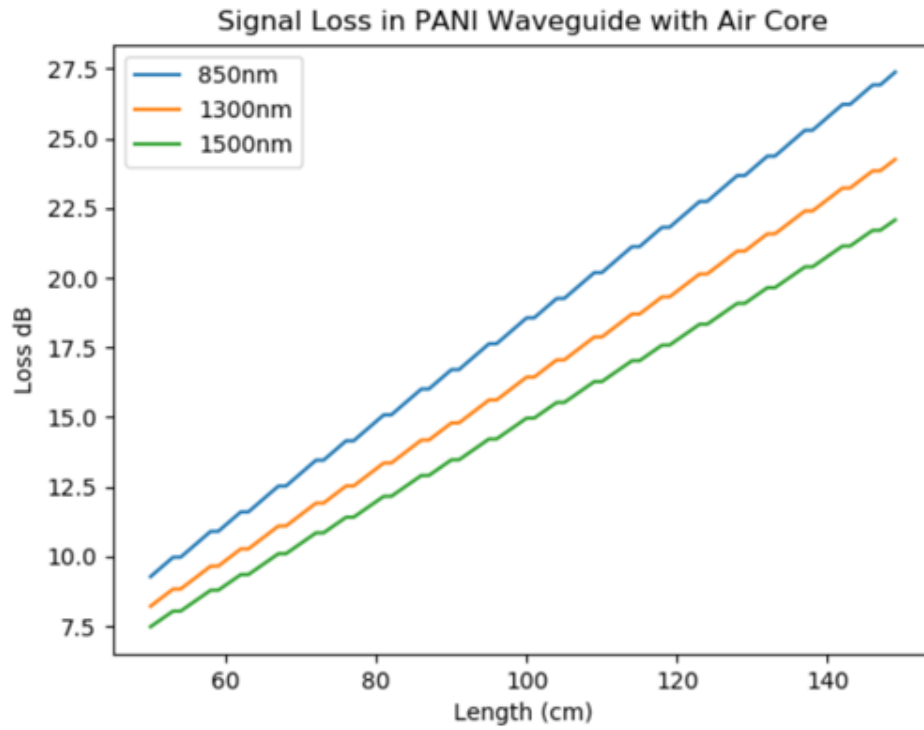


Figure 7.18 Signal loss of NIST suggested wavelengths in IR- range in waveguides with PANI and SiO₂/Air systems vs length (distance travelled).

CHAPTER 8

APPLICATIONS AND FUTURE WORK

In the modern world, we cannot survive without the incredibly large class of materials we know as polymers. They play a vital role in our daily lives by being incorporated in almost everything and their impact on the present way of life and the global economy is almost incalculable. They are a distinct class of materials that have applications in almost all fields of technology that are as diverse as drug delivery systems to avionics. They are advantageous to use as they have many pros such as below average cost, ease of manufacturing, tunability, flexibility, light weight etc. These positive features encourage further development in research in many diverse areas. Thus, we cannot confine the study of polymers as a single, specialized interdisciplinary field but rather a specialized, broad and unique discipline that includes parts of chemistry, physics, biology, materials, engineering and several other scientific fields.

8.1 Sensors

Smart materials are substances that respond to an external stimulus from its environment which can be physical or chemical that results in a specific reproducible and usable change in material properties. Polymers can be termed as smart materials because their physical and chemical properties make them versatile candidates for many applications. In the last several years, it has been discovered that some polymeric materials could reversibly or irreversibly change their physical and chemical properties under the influence of external stimuli, e.g., pH, temperature, presence of specific ions, light radiation, mechanical forces,

magnetic fields, electric fields, and bioactive molecules. Smart polymers can be applied to solve complex issues such as controlled delivery of drugs and genes, catalysis, detection and imaging, adaptive coatings, or self-healing materials in various forms such as solutions, films, solids, etc. (Cichosz et al. 2018).

In the last two decades, polymer-based sensors have been researched vigorously and it has found many useful applications in various fields. The enforcement of stricter legislative environmental acts has magnified the demand for the establishment of materials/equipment to monitor factors that can endanger human life, such as the presence of toxic gas or vapors, water pollution, pesticides, etc. Once they are established as biocompatible, these polymers can be used in the medical field. Overall, polymers have many adaptable properties and features that can be enhanced with appropriate modification or synthesis methods and thus they are an attractive choice of material for sensory applications (Cichosz et al. 2018).

Fluorescent polymer thermometers were first created in the early 2000s by mixing polarizable fluorescent dyes and polymers that can aggregate. Aqueous solutions of high molecular weight polymers are used to make the matrix such as N-isopropylacrylamide (NIPAM), N-isopropylmethacrylamide (NIPMAM), N-propylacrylamide (NNPAM), and N-tert-butylacrylamide (NTBAM). Benzoxadiazole-containing compounds, such as 4-N-(2-acryloyloxyethyl)-N-methylamino-7-(N,N-dimethylamino) sulfonyl-2,1, benzoxadiazole (DBDAE) are used as pigments in the color changing temperature sensitive sensor. The polymers tend to aggregate and reduce their polarity above their lower critical solubility temperature which ultimately makes the microenvironment of the dyes change from hydrophilic to hydrophobic. The dyes have poor fluorescence in hydrophilic

environments and high intensity fluorescence in hydrophobic environments. Thus, the formation of polymer aggregates due to temperature changes causes the dyes to fluoresce and act as a functional sensor (Cichosz et al. 2018).

pH sensors are required to determine the pH during the manufacture of a variety of products. Photochemical polymerizable copolymers such as acrylamide and methylene-bis-acrylamide have been used to make these sensors but polyaniline (PANI) is also a popular choice for sensors that function in aqueous media. Commercially used blood pH sensors which function as electrodes are also available. Polymer thin films that exhibit high sensitivity to hydronium ion concentration changes have also been developed using poly(2-hydroxyethyl methacrylate) and 2-dimethylaminoethyl methacrylate. Poly(p-phenylenediamine) (PPV) has been shown to exhibit photoconductive properties which makes it a promising material for electronic applications and thus can be implemented in modern pH sensors (Cichosz et al. 2018).

This same concept of potential electrode changes due to changes in the environment can be used to detect the presence of gases. Conductive polymers and composites with polymers such as PVC and PMMA have found applications in gas sensing devices. They can also be used as moisture and humidity sensors which are required to monitor air quality in many areas, such as industry, medicine, or a household (Cichosz et al. 2018).

Table 8.1 Examples of Different Types of Polymeric Gas Sensors

Polymer	Application	Properties
poly(vinyl chloride)	detection of pethidine hydrochloride in suppositories and tablets	association of pethidine phosphate ions
Polystyrene and polyisoprene	control of organic pollution	piezoelectric effect
copolymers of butyl and methacrylates	measurements of copper ion content	polymer paste used to create ion-selective membranes
hydrophobic polymers	detection of organic contaminants in drinking water	formation of susceptible coatings
Polyaniline	moisture sensor, NH ₃ , NO ₂	possibility of creating ultra-thin films
Polyester	detection of H ₂ O ₂	possibility of creating composite materials for electrodes

Ion selective sensors have been created to detect the presence of specific ions in solution that has a mixture of dissolved ions. Silicone rubber and PU/PVC copolymer membranes have been used to detect sodium ions in body fluids. PANI can be used to detect calcium ions by transforming ionic reactions to electrical signals. Poly(vinyl chloride) (PVC), poly(3,4-ethylenedioxythiophene) (PEDOT) and crosslinked poly(ethylene glycol) (PEG) are also popular choices as they allow for faster signal generation and better stabilization after injecting the analyte and they are also biocompatible and thus have applications in medical devices (Cichosz et al. 2018).

Stress sensors are made of polymers that exhibit photoluminescence, color changes or fluorescence emissions that are dependent on the deformation the material undergoes

when exposed to various forces such as shearing or stretching. Research in this area is relatively new but several candidates that would be ideal for these applications have been identified such as oligo(p-phenylene vinylene) used as a dye in low density polyethylene (LDPE), compound based on poly(methyl acrylate) (PMA) with introduced spiropyran moieties within polymer chains, etc. (Cichosz et al. 2018).

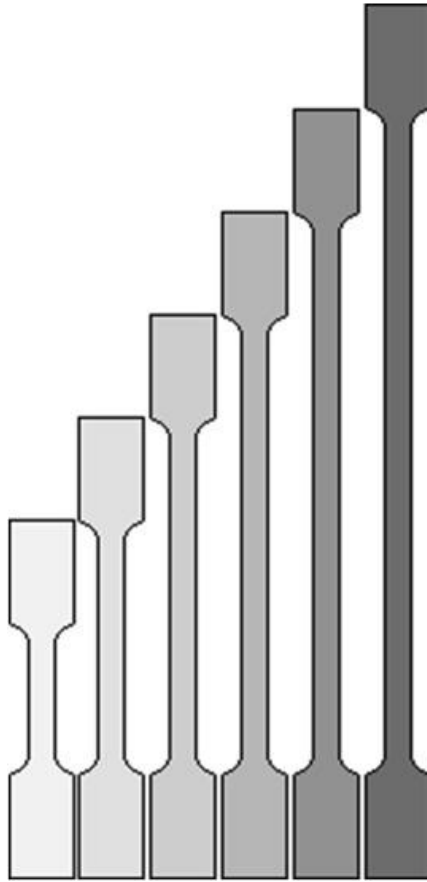


Figure 8.1 Schematic color changes of an extended sample used to make stress sensors.

Stress sensors can also have medical applications. They can be used for cardiac recordings that monitor blood pressures near or at the surface of skin and thus give accurate and reliable results of the heart rate (Cichosz et al. 2018).

Biosensors are used to quantify a biological reaction by transforming it into a measurable electrical signal. They are composed of three elements: a biological component, a bioreceptor and a polymer sensor. They have applications in many fields such as medical diagnostics and environmental pollution control. When a biological reaction occurs, the product diffuses into the sensor which induces changes in the material's electrical properties and thus it generates a signal that can be read by a detector (Cichosz et al. 2018).

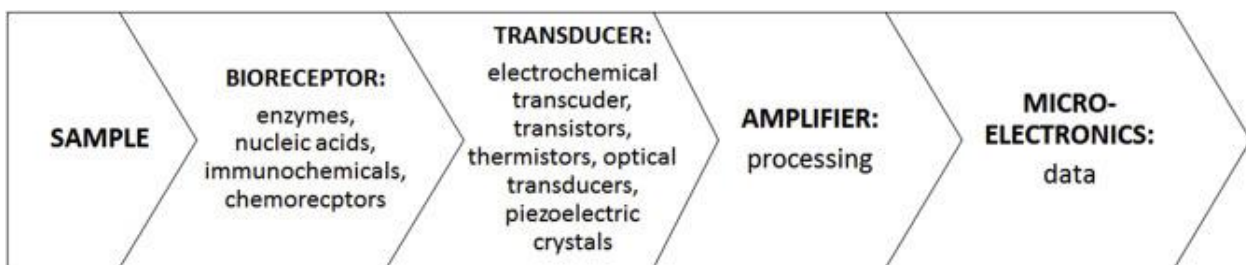


Figure 8.2 Principle of operation of a biosensor.

Table 8.2 Different Types of Polymeric Biosensors

Polymer	Application	Properties
cellulose membranes with bacterial origin	glucose sensor	increasing and prolonging stability
poly(vinyl chloride)	analysis of creatine in urine	polymer membrane with natural electrically inert lipids applied as plasticizers

Polymer	Application	Properties
Polyaniline	glucose, urea, triglyceride sensor	polymer deposition and enzymatic immobilization controlled electrochemically
poly(o-aminophenol)	glucose biosensors	amperometric sensor on platinized glassy carbon electrode
Polypyrrole	glucose detection	electrode immobilization of enzymes by electropolymerization of pyrrole
Polyamine	L-amino acid sensor	Immobilization of enzymes by electropolymerization
redox polymers capable of crosslinking	biosensors for enzymes	use of polymers with an ability to cross-link

8.2 Organic Photovoltaic (OPV) Solar Cells

As the need for clean, renewable energy sources broadens, polymer solar cells provide exciting possibilities to address these issues. Polymer solar cells are advantageous to use because of their printability which allows for much easier fabrication of devices. Production and manufacturing of these devices have the potential to be commercialized in a continuous printing process. Various printing and coating technologies have been shown to be compatible with semiconducting polymer processing (Cai et al. 2010)

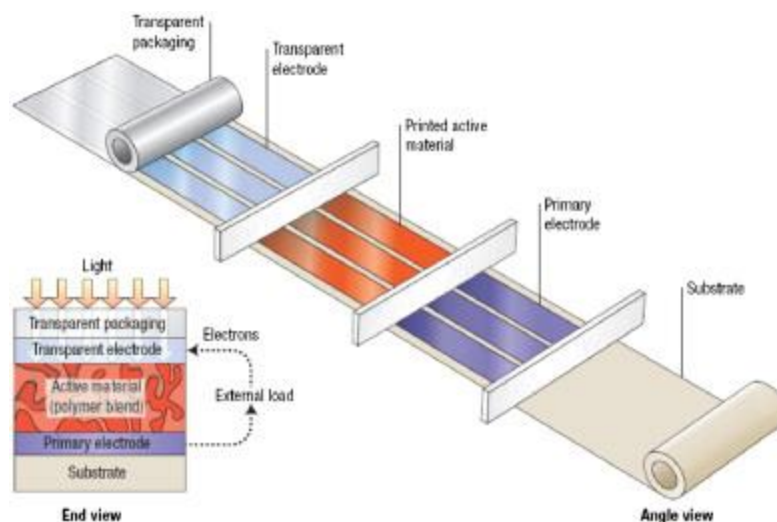


Figure 8.3 Schematic illustration of how polymer solar cells are manufactured by standard printing processes.

Current power conversion efficiency (PCE) of polymer solar cells are about one third of rigid inorganic photovoltaic cells such as silicon-based devices which make them unideal for present day applications. However, flexibility, light weight and ease of manufacture make polymers worthy of being investigated to improve their performance.

Polymer solar cells have a bilayer structure with an electron donor and an electron acceptor on top of each other which form the p-n junction. This structure is sandwiched between the conductive electrodes and as they have different electron affinities and ionization energies, electrostatic forces are produced at the interface of the two layers. Issues that arise from this structure is that the diffusion length of the charge carriers or excitons are extremely short, which limits the thickness of the layers. This in turn makes the cell inefficient as they cannot absorb as much energy as a thicker layer like those present in inorganic solar cells. To make polymer solar cells more efficient, a bulk heterojunction layer is used which is a blend of the p and the n-type material with domains in the nanoscale which allows excitons with short lifetimes to reach the interface. This allows for the layer

to be thicker and thus more efficient. The formation and optimization of this layer is critical to the functionality of polymer solar cells.

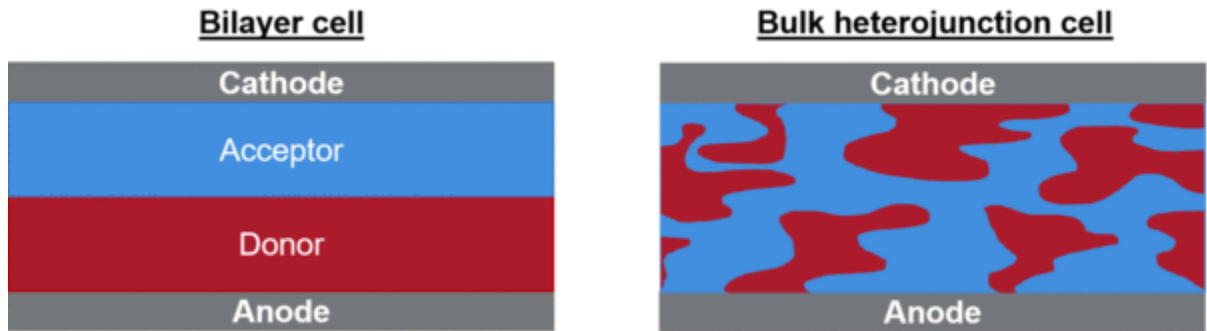


Figure 8.4 A comparison of the originally proposed bilayer cell, and the modern bulk heterojunction cell

In modern research, most of the OPVs used are solution-processed BHJ cells. PEDOT:PSS paired with an ITO anode is a commonly used material for the hole-transporting layer (HTL) and calcium paired with an aluminum cathode is used as an electron-transporting layer (ETL). These layers boost the movement of one type of charge through favorable energy level positioning and blocking the movement of the other carrier ("Organic Photovoltaic (OPV) Cells | How Organic Solar Cells Work").

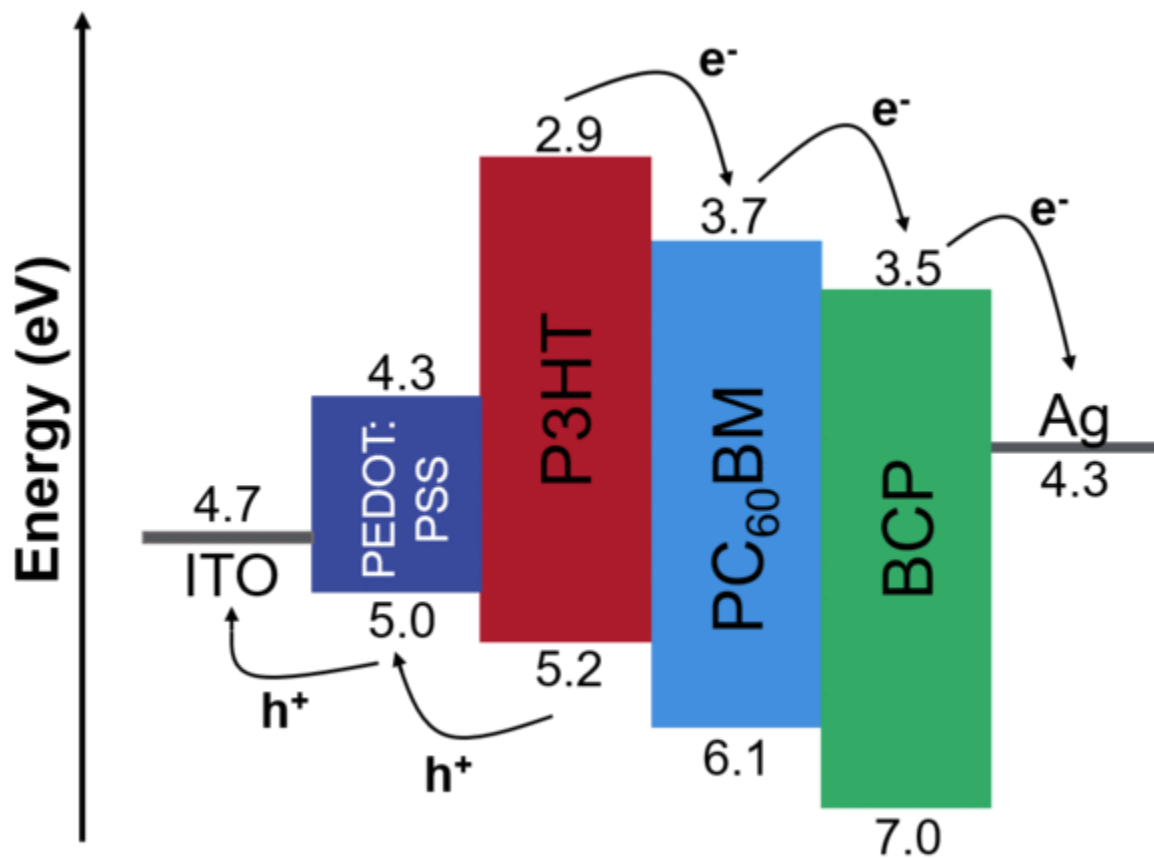


Figure 8.5 An approximation of charge carrier transport in the full stack of a conventional OPV, using the organic molecule BCP as an ETL. The smooth movement of energy levels facilitating transport is known as a bandgap cascade.

Fullerene derived acceptors (usually in the form of PCBM) have been used traditionally in polymer solar cells; however, there has been a shift towards non-fullerene acceptors (NFAs) as they have higher efficiencies and stabilities. Typical fullerene acceptors have lower absorption in the visible spectrum but NFAs have been produced to have more efficient absorbance which allows for higher exciton production in both components of the active layer. High performance polymer donor material includes PBDB-T and PTB7 ("Organic Photovoltaic (OPV) Cells | How Organic Solar Cells Work").

Other than the inefficiency of OPVs due to insufficient energy of light entering the device, higher absorbed energies, larger than the band gap, causes energy loss due to thermalization of the electron, entropic losses, and radiative recombination. BHJ morphology, narrow absorption, reduced charge carrier transport and mobility, and high recombination leading to voltage losses are other limitations that need to be addressed to improve efficiencies. Further research also needs to be done on scalability and long-term stability to achieve OPV commercialization ("Organic Photovoltaic (OPV) Cells | How Organic Solar Cells Work").

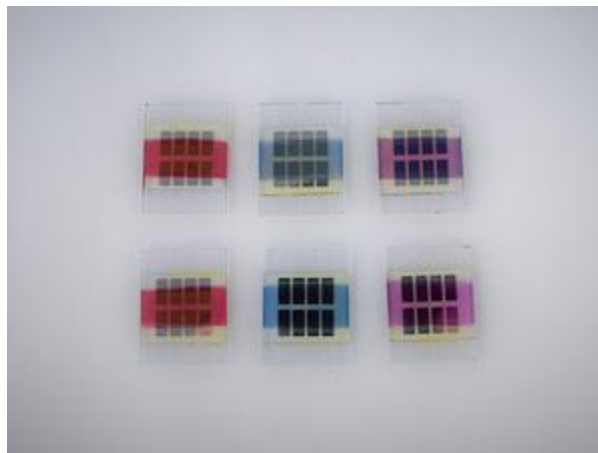


Figure 8.6 Laboratory OPV cells manufactured on glass.

8.3 Coatings

Coatings can alter surface properties of materials to enhance their performance and make them more applicable in various technical fields. Polymer coatings have been used for purposes of adhesion, barrier properties, scratch and abrasion resistance, chemical resistance, wettability, biocompatibility, etc. Various techniques have been established to create protective organic coatings. The right choice of material, coating method and

fabrication parameters are necessary to create high performance coatings with desired characteristics. Polymer coatings have been successfully implemented in various applications such as solar cells, lithium-sulfur batteries, membrane technology, Light-Emitting Diodes, corrosion protection, packaging, and biomedical devices (Smith and Lamprou 2014).

In the field of biomedical applications, polymer coatings have a plethora of functionalities that can be harnessed for diverse uses such as wear-resistance, improved mechanical strength, corrosion protection, enhanced biocompatibility, electrical conductivity and tailored surface chemistry (Smith and Lamprou 2014). These coatings can be as simple as basic barrier coatings to sophisticated nano-technology based composites.

Orthopedic implantable devices are often made of alloys of magnesium or titanium due to their many attractive characteristics such as non-toxic corrosion products, low density, good fracture toughness, elastic moduli and compressive yield strengths that are similar to biological bone tissue. To reduce corrosion rates in Mg based alloys, it can be coated with conducting polymer poly(3,4-ethylenedioxythiophene) (PEDOT). Studies have also been conducted on poly(L-lactide) (PLLA) and semi-crystalline poly(ϵ -caprolactone) (PCL) as electrospun or dip-coated films for MG based alloys and it was found that they both reduced the corrosion rate and increased cytocompatibility by promoting better cell attachment. Titanium alloys have the tendency to fail because of bacterial infection and poor osseointegration. This can be combated by coating the device with biodegradable and antibacterial polymers such as chitosan and PLGA which also have drug-eluting properties (Smith and Lamprou 2014).

A wide variety of materials are available for multiple applications in the engineering field; however, a very few are practical. All materials are exposed to multiple external stimuli such as thermal, mechanical, chemical stresses or radiation, which make them susceptible to damage. This can lead to structural degradation and internal crack formation, which alter the physical and mechanical properties of the material. When structural materials are impaired, there are very few ways the “device” can be conserved so that its functional lifetime can be extended. Ideally, the material would repair itself by continuously sensing external stimuli and respond to the damage caused accordingly. This makes the material durable, more reliable, easier to maintain and reduce repair costs. Therefore, there is a need to develop “smart” materials (Hossain and Ravindra, 2019).

Conventional methods of repairing materials include welding (reformation of surface bonds at site of fracture by heat, infrared or other external stimulation) or patching (replacement or covering/coating with different material at site of fracture). However, these methods have inadequate reliability as the location of repair is still the weakest point in the material thus making it likely to fail again. Materials with the ability to heal autonomously and consistently at the molecular level without the need for external intervention are thus required to mitigate these issues (Hossain and Ravindra. 2019).

The ideal self-healing material should have several characteristics that make it technologically and economically appealing. S. van der Zwaag defined the terms for the ideal material and a minimal self-healing material. The ideal material should be able to heal damage of any size completely and limitlessly without the need for external intervention (autonomously). The healed site should have equal or superior properties to the original matrix and should be cost-effective. A minimal self-healing material (a more

realistic situation) is able to heal small instances of damage partially and at least once. It might need external stimulation to induce the healing process and the healed site has properties that are inferior to host matrix and the material is not cost-effective. In practice, the performance of healed materials decreases with time as demonstrated in Figure 8.7 (Hossain and Ravindra, 2019).

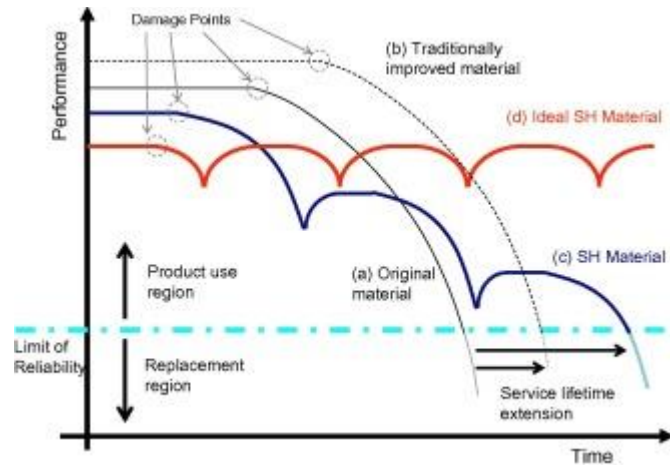


Figure 8.7 Lifetime extension of engineered materials by implementation of self-healing principle.

Autonomic healing materials that respond to external stimuli in a non-linear and productive way have immense potential for advanced engineering systems especially in corrosion resistance. Many different strategies have been successfully implemented to achieve repair of bulk mechanical damage as well as dramatic increases in the fatigue life such as encapsulation, reversible chemistry, microvascular networks, nanoparticle phase separation, polyionomers, hollow fibers, and monomer phase separation. However, due to chemical and physical limitations, these approaches are difficult to implement as coatings. Polymeric coatings protect the substrate from environmental contaminants that can cause corrosive reactions but as they are very thin and in direct contact with the surroundings, the coating itself will have negative exposure to the contaminants. (Cho et al. 2009)

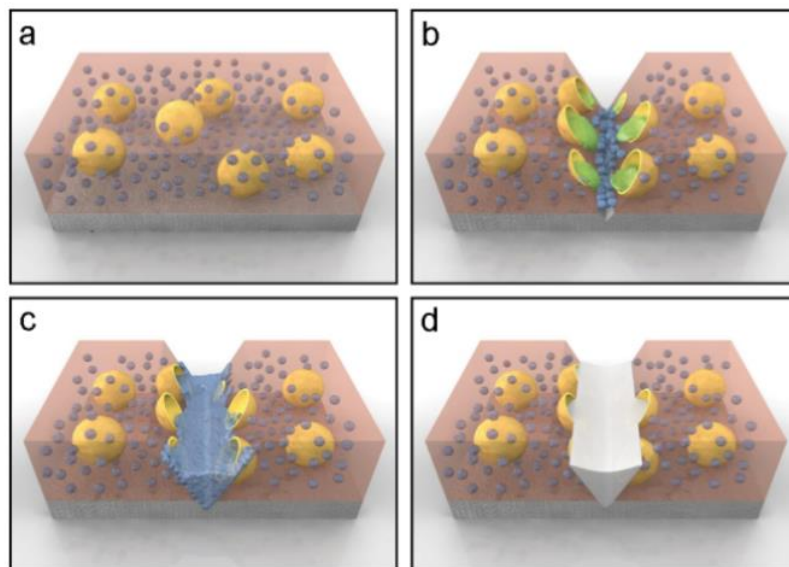


Figure 8.8 Schematic of self-healing process. a) Self-healing coating containing microencapsulated catalyst (yellow) and phase-separated healing agent droplets (blue) in a matrix (light orange) on a metallic substrate (grey). b) Damage to the coating layer releases catalyst (green) and healing agent (blue). c) Mixing of healing agent and catalyst in the damaged region. d) Damage healed by cross-linked PDMS, protecting the substrate from the environment.

Cho et al. from Beckman institute showed that di-n-butyltin dilaurate catalyzed polycondensation of hydroxyl end-functionalized polydimethylsiloxane (HOPDMS) and polydiethoxysiloxane (PDES) exhibited self-healing chemistry which was stable in the presence of contaminants such as water and oxygen and it remained active at temperatures up to 150 °C thus allowing it to be implemented in systems that require thermal curing (Cho, et al. 2009).

8.4 Energetic materials

Nitrocellulose is a low-cost, mass-manufactured material that is employed in the production of gun propellant fabrication for the DoD and commercially. It has the potential

to be used as a combustible cartridge case material in large caliber weapon systems for easy transport and operation of gun propulsion charges during gun firing. These cases can protect the energetic charges and be completely expended during the interior ballistic cycle in any weapon platform. Knowing the emissivity of a surface can be utilized in many ways such as accurate non-contact temperature measurement and for heat transfer calculations. In 2019, Elbert Caravaca and group did a review on the correlation between emissivity and the combustion behavior of a material and found evidence of an existing relationship. Further research needs to be conducted to obtain detailed information on this matter. Currently, not much has been done to determine on the influence of emissivity on the combustion behavior of materials but some research has been done to correlate the emissivity of materials to chemical reaction kinetics. Time to ignition is also shown to be influenced by emissivity of the material (Caravaca et al. 2019).

8.5 Future work

Sustainable, biodegradable and “green” products are increasing in popularity, as evidenced by the growth in green labeling initiatives, eco-marketing, and bio-based materials. Polymers are incredibly stable materials that take decades to completely disintegrate. They have a multiple negative impacts on not only the environment but also our health. It is our responsibility to invest in further research to improve biodegradability, non-toxicity and maximize efficiency of these materials to reduce the impact they have on our environment. However, polymers are also very beneficial to our livelihoods. They can enable the purification of water or can be utilized as polymer composites with improved fuel economy

for aerospace applications. They can also be derived from biomass instead of petrochemicals thus reducing some of their environmental impact (Tabone, et al. 2010).

Future work in the field of sustainable design metrics should include the discussion of available data during the design phase of chemical products. In future quantitative assessments of green design methods, data such as the toxicity of reactants and the heat of reaction can be used to measure adherence principles such as to reduce energy consumption and avoid hazardous chemicals. Such tools can be designed to apply existing life cycle assessment data to nascent chemical design; they can increase the awareness of green chemists and aid the development of more environmentally beneficial chemical products. (Tabone, et al. 2010)

REFERENCES

Adve, R.S., et al. "Application of the Cauchy method for extrapolating/interpolating narrowband system responses." *IEEE Transactions on Microwave Theory and Techniques*, vol. 45, no. 5, 1997, pp. 837-845.

Balani, Kantesh, et al. *Biosurfaces: A Materials Science and Engineering Perspective*. John Wiley & Sons, 2015.

Cai, Wanzhu, et al. "Polymer solar cells: Recent development and possible routes for improvement in the performance." *Solar Energy Materials and Solar Cells*, vol. 94, no. 2, 2010, pp. 114-127.

Caravaca, Elbert, et al. "Effects of Emissivity on Combustion Behavior of Energetic Materials." *TMS 2019 148th Annual Meeting & Exhibition Supplemental Proceedings*, 2019, pp. 1629-1641.

Cho, Soo H., et al. "Self-Healing Polymers: Self-Healing Polymer Coatings (Adv. Mater. 6/2009)." *Advanced Materials*, vol. 21, no. 6, 2009, pp. NA-NA.

Cichosz, Stefan, et al. "Polymer-based sensors: A review." *Polymer Testing*, vol. 67, 2018, pp. 342-348.

"Dielectric Properties." *CROW*,
polymerdatabase.com/polymer%20physics/Permittivity.html.

Dr. Rüdiger Paschotta. "Page Not Found." *RP Photonics Consulting GmbH - Technical Consulting on Laser Technology, Nonlinear Optics, Fiber Optics; Simulation and Design Software; Encyclopedia and Buyer's Guide*, 24 Mar. 2019, www.rp-photonics.com/refractive_index.htm.

Elkomy, G.M., et al. "Structural and optical properties of pure PVA/PPY and cobalt chloride doped PVA/PPY films." *Arabian Journal of Chemistry*, vol. 9, 2016, pp. S1786-S1792.

Fried, Joel R. *Polymer Science and Technology*. Pearson Education, 2014.

Hakim, Hussein, et al. "STUDY THE OPTICAL PROPERTIES OF POLYVINYLPIRROLIDONE (PVP) DOPED WITH KBr." *European Scientific Journal*, vol. 3, Dec. 2013.

Hall, Christopher. "Electrical and Optical Properties." *Polymer Materials*, 1981, pp. 92-112.

Kailas, Satish V. "Optical properties." *NPTEL*, Indian Institute of Science, nptel.ac.in/courses/112108150/pdf/Web_Pages/WEBP_M17.pdf.

Krivokhvos, Olga. "Conventional and nonconventional Kramers-Kronig analysis in optical spectroscopy." 2014. Lappeenranta University of Technology, MS thesis.

MacDiarmid, A. G., et al. "The Concept of 'Doping' of Conducting Polymers: The Role of Reduction Potentials [and Discussion]." *Philosophical Transactions of the Royal Society A: Mathematical, Physical and Engineering Sciences*, vol. 314, no. 1528, 1985, pp. 3-15.

Namazi, Hassan. "Polymers in our daily life." *BioImpacts*, vol. 7, no. 2, 2017, pp. 73-74.

"Organic Photovoltaic (OPV) Cells | How Organic Solar Cells Work." *Ossila*, www.ossila.com/pages/organic-photovoltaics-introduction.

"Refractive Index." *Physics: Problems and Solutions*, physics.fandom.com/wiki/Refractive_index.

Smirnov, José R., et al. "Flexible all-polymer waveguide for low threshold amplified spontaneous emission." *Scientific Reports*, vol. 6, no. 1, 2016.

Smith, J. R., and D. A. Lamprou. "Polymer coatings for biomedical applications: a review." *Transactions of the IMF*, vol. 92, no. 1, 2014, pp. 9-19.

Sreekanth, K., et al. "Optical and electrical conductivity studies of VO₂+ doped polyvinyl pyrrolidone (PVP) polymer electrolytes." *Journal of Science: Advanced Materials and Devices*, vol. 4, no. 2, 2019, pp. 230-236.

Swatowski, Brandon. "POLYMER WAVEGUIDE MANUFACTURING AND PRINTED CIRCUIT BOARD INTEGRATION." 2017. Michigan Technological University, MS thesis.

Tabone, Michaelangelo D., et al. "Sustainability Metrics: Life Cycle Assessment and Green Design in Polymers." *Environmental Science & Technology*, vol. 44, no. 21, 2010, pp. 8264-8269.

Taha, T. A., et al. "Effect of NiO NPs doping on the structure and optical properties of PVC polymer films." *Polymer Bulletin*, vol. 76, no. 9, 2018, pp. 4769-4784.

"Wave Behavior and Interaction | Boundless Physics." *Lumen Learning – Simple Book Production*, courses.lumenlearning.com/boundless-physics/chapter/wave-behavior-and-interaction/.

"What is Emissivity and Why is It Important?" *National Physical Laboratory - NPL*, www.npl.co.uk/resources/q-a/why-is-emissivity-important.